

Non-Gaussian wave functionals in Coulomb gauge Yang-Mills theory

Davide R. Campagnari and Hugo Reinhardt

Institut für Theoretische Physik, Universität Tübingen, Auf der Morgenstelle 14, 72076 Tübingen, Germany

(Received 27 September 2010; published 18 November 2010)

A general method to treat non-Gaussian vacuum wave functionals in the Hamiltonian formulation of a quantum field theory is presented. By means of Dyson-Schwinger techniques, the static Green functions are expressed in terms of the kernels arising in the Taylor expansion of the exponent of the vacuum wave functional. These kernels are then determined by minimizing the vacuum expectation value of the Hamiltonian. The method is applied to Yang-Mills theory in Coulomb gauge, using a vacuum wave functional whose exponent contains up to quartic terms in the gauge field. An estimate of the cubic and quartic interaction kernels is given using as input the gluon and ghost propagators found with a Gaussian wave functional.

DOI: [10.1103/PhysRevD.82.105021](https://doi.org/10.1103/PhysRevD.82.105021)

PACS numbers: 11.10.Ef, 12.38.Aw, 12.38.Lg

I. INTRODUCTION

According to our present understanding of nature, QCD is the theory of the strong interaction. This theory has been tested in the high-momentum or ultraviolet (UV) regime, where perturbation theory is applicable due to asymptotic freedom. Our knowledge on the low energy, strongly interacting regime of QCD stems mainly from lattice calculations, which have at least qualitatively reproduced many physical observables, in particular, the linearly rising confining potential for heavy quarks. Furthermore, lattice calculations have revealed the relevance of topological field configurations such as magnetic monopoles and center vortices for infrared phenomena like confinement and spontaneous chiral symmetry breaking. These calculations support the dual Meissner effect and the vortex condensation picture of confinement [1]. Despite these substantial physical insights provided by the lattice calculations, a thorough understanding of these infrared phenomena will not come from lattice calculations alone but will require also studies of the continuum theory.

In recent years there have been substantial efforts devoted to a nonperturbative treatment of continuum Yang-Mills theory. Among these are a variational solution of the Yang-Mills Schrödinger equation in Coulomb gauge [2–5]. In this approach, using Gaussian-type wave functionals, minimization of the energy density results in the so-called gap equation for the gluon energy (or static gluon propagator). This equation has been solved analytically in the infrared [6] and in the ultraviolet [7] and numerically in the full momentum regime [4,8]. One finds a gluon energy, which in the UV behaves like the photon energy but diverges in the IR, signalling confinement. The obtained gluon energy also compares favorably with the lattice data [9]. In particular, the infrared regime is correctly reproduced, as far as we can tell from available lattice data. There are, however, deviations in the midmomentum regime (and minor ones in the UV) which can be attributed to the missing gluon loop, which escapes the Gaussian

wave functionals. These deviations are presumably irrelevant for the confinement properties, which are dominated by the ghost loop (which is fully included under the Gaussian ansatz), but are believed to be important for a correct description of spontaneous breaking of chiral symmetry [10].

The numerical wave functional obtained from the variational solution of Ref. [8] seems to embody the correct infrared physics as is revealed in the various applications considered to date: One finds a linearly rising static quark potential [8], an infrared enhanced running coupling constant with no Landau pole [6], a topological susceptibility in accord with lattice data [11], a perimeter law for the 't Hooft loop [12], and, within an approximate Dyson-Schwinger equation, an area law for the spatial Wilson loop [13]. Furthermore, in Ref. [14] it was shown that the inverse ghost form factor of Coulomb gauge Yang-Mills theory represents the dielectric function of the Yang-Mills vacuum and the so-called horizon condition [15] (of an infrared diverging ghost form factor) implies that the Yang-Mills vacuum is a perfect color dielectricum, i.e., a dual superconductor, which establishes the connection between the Gribov-Zwanziger confinement scenario [15,16] and the monopole condensation picture [17,18]. Finally, in Ref. [19] the functional renormalization group flow equation of the Hamiltonian approach to Coulomb gauge Yang-Mills theory was studied, yielding results for the gluon and ghost propagator similar to that of the variational approach [4].

In the present paper, we generalize the variational approach to the Hamiltonian formulation of Yang-Mills theory to non-Gaussian wave functionals. We will present a general method to treat non-Gaussian wave functionals in quantum field theory. The method is based on the observation that expectation values in the Hamiltonian formulation of $d = 3 + 1$ -dimensional quantum field theory can be formally obtained from a generating functional of $d = 3$ -dimensional Euclidean quantum field theory with an action defined by the logarithm of the vacuum wave

functional. Expanding this action functional in powers of the underlying field results in “bare” n -point kernels γ_n as expansion “coefficients.” We then exploit Dyson-Schwinger equation (DSE) techniques [20–22] to express the expectation value of the Hamiltonian $\langle H \rangle$ in terms of these kernels γ_n , which are then determined by the variational principle, i.e., by minimizing $\langle H \rangle$. This approach is then applied to the Hamiltonian formulation of Yang-Mills theory in Coulomb gauge to include three- and four-gluon interaction kernels in the exponent of the Yang-Mills vacuum wave functional.

By using such a non-Gaussian wave functional, the gluon loop is retained in the expectation value of the Hamiltonian. Although the gluon loop is irrelevant for the IR properties, it certainly influences the midmomentum and UV regime of the gluon propagator, and thus of the running coupling, and also contributes to the anomalous dimensions. As a first estimate of the effects of the non-Gaussian terms in the wave functional, we will calculate the gluon-loop contribution to the gluon propagator as well as the three- and four-gluon proper vertices using the ghost and gluon propagators obtained from the Gaussian wave functional [8] as input. A full self-consistent inclusion of the three- and four-gluon vertices will be the subject of future research.

It is clear from the very beginning that eventually we have to truncate the tower of DSEs for the proper n -point vertex functions Γ_n as well as the equations of motion for the variational kernels γ_n following from the variational principle. For a systematic counting of the various diagrams we will assume a skeleton expansion.

Previous variational calculations (using Gaussian wave functionals) were restricted to two (overlapping) loops in the energy $\langle H \rangle$, resulting in a one-loop gap equation for the gluon propagator. Restriction to two overlapping loops in the energy results in a bare (zero-loop) three-gluon kernel γ_3 and in a vanishing four-gluon kernel $\gamma_4 = 0$. To get a $\gamma_4 \neq 0$, one has to include up to three loops in the energy. To keep the calculation sufficiently simple, we will keep only those three (overlapping) loop terms in the energy containing three- or four-gluon kernels. This will result in a bare (zero-loop) four-gluon and a one-loop three-gluon vertex.

The organization of the paper is as follows: In Sec. II we present the DSEs of the Hamiltonian approach first for a general field theory and afterwards for Yang-Mills theory in Coulomb gauge. The full static (equal-time) propagators of the Hamiltonian approach are expressed in terms of proper vertex functions in Sec. III. In Sec. IV we specify our Yang-Mills vacuum wave functional and derive the corresponding DSEs for the gluon and ghost proper n -point functions. By means of these DSEs, the vacuum expectation value of the Hamiltonian is expressed in Sec. V in terms of the variational kernels of the vacuum wave functional. In Sec. VI these kernels are determined by

minimizing the energy density. Finally, in Sec. VII we calculate the three- and four-gluon proper vertices using as input the ghost and gluon propagators from the variational calculations with a Gaussian wave functional. A short summary and our conclusions are given in Sec. VIII.

II. DYSON-SCHWINGER EQUATIONS OF THE HAMILTONIAN APPROACH TO YANG-MILLS THEORY IN COULOMB GAUGE

A. General DSE formalism of the Hamiltonian approach to quantum field theory

Consider a quantum field theory comprised of a collection of fields $\phi = (\phi_1, \phi_2, \dots)$ and let $|\psi\rangle$ be the exact vacuum state. All static (time-independent) Green’s functions, i.e., vacuum expectation values $\langle \phi \phi \dots \rangle$, can be calculated from the generating functional

$$Z[j] = \langle \psi | e^{\int j \cdot \phi} | \psi \rangle, \quad (1)$$

where $j = (j_1, j_2, \dots)$ stands for the collection of sources corresponding to the fields and we use the abbreviation $j \cdot \phi = j_1 \phi_1 + j_2 \phi_2 + \dots$. In the “coordinate” representation of the vacuum state $\langle \phi | \psi \rangle = \psi[\phi]$, the scalar product in (1) is defined by the functional integral over time-independent fields $\phi(\mathbf{x})$:

$$Z[j] = \int \mathcal{D}\phi |\psi[\phi]|^2 e^{\int j \cdot \phi}. \quad (2)$$

Furthermore, the integral in the exponent is over spatial coordinates \mathbf{x} of the static fields $\phi(\mathbf{x})$. Expressing the vacuum wave functional in the form¹

$$\psi[\phi] = \exp(-\frac{1}{2}S[\phi]), \quad (3)$$

the generating functional of the Hamiltonian approach to quantum field theory becomes

$$Z[j] = \int \mathcal{D}\phi e^{-S[\phi] + \int j \cdot \phi}, \quad (4)$$

which is a standard generating functional of the $d = 3$ -dimensional Euclidean quantum field theory defined by an “action” $S[\phi]$. Here, this action is defined by the vacuum wave functional $\psi[\phi]$ and will, in general, be nonlocal and nonlinear. We therefore perform a Taylor expansion of the action functional $S[\phi]$ in powers of the time-independent fields $\phi(\mathbf{x})$. The constant part $S[0]$ is fixed by the normalization of the wave functional and the linear part can be absorbed into the external source. It is then sufficient to consider expansions of $S[\phi]$ starting at second order:

¹As long as we ignore the θ vacuum of Yang-Mills theory, the vacuum wave functional can be chosen to be real, which we will assume in the present paper.

$$S[\phi] = \frac{1}{2} \int \gamma_2 \phi^2 + \frac{1}{3!} \int \gamma_3 \phi^3 + \dots \quad (5)$$

Restricting the expansion to second order yields a Gaussian wave functional (3) for which the functional integral in Eq. (2) can be explicitly carried out. This corresponds to the so-called mean-field approximation, where all higher-order Green's functions of the field $\phi(\mathbf{x})$ are given in terms of the propagator $\langle \phi \phi \rangle$.

In many cases the mean-field approximation is, however, not sufficient. Going beyond the mean-field approximation, the functional integral in (2) can no longer be explicitly performed. However, we can calculate the desired Green functions by exploiting Dyson-Schwinger equation techniques. Starting from the identity

$$\int \mathcal{D}\phi \frac{\delta}{\delta\phi} (e^{-S[\phi] + \int j\phi}) = 0, \quad (6)$$

we can derive, in the standard fashion, a set of DSEs for the Green functions $\langle \phi \phi \dots \rangle$. This infinite tower of equations has to be truncated to get a closed system of equations, and further simplifying assumptions on the form of the interaction kernels γ_n entering the ansatz for the vacuum wave functional [see Eqs. (3) and (5)] will be required. Nevertheless, this approach allows us to go beyond Gaussian wave functionals and calculate the static Green functions $\langle \phi \phi \dots \rangle$ in terms of the kernels γ_n . By means of these static Green functions, the vacuum expectation value of the Hamiltonian $\langle \psi | H | \psi \rangle$ is expressed in terms of the kernels γ_n , which are then found by minimizing the energy density.

In the Hamiltonian approach to quantum field theory one is not primarily interested in the generating functional (2) itself but in expectation values of observables, in particular, of the Hamiltonian. For this purpose it turns out to be more convenient to generalize Eq. (6) to

$$\int \mathcal{D}\phi \frac{\delta}{\delta\phi} (e^{-S[\phi]} K[\phi]) = \int \mathcal{D}\phi \frac{\delta}{\delta\phi} (\psi^*[\phi] K[\phi] \psi[\phi]) = 0, \quad (7)$$

where $K[\phi]$ is an arbitrary functional of the underlying field ϕ .

B. Derivation of the DSEs for the Hamiltonian approach to Yang-Mills theory in Coulomb gauge

Below, we apply the general Dyson-Schwinger approach to the Hamiltonian formulation of quantum field theory outlined above to Yang-Mills theory in Coulomb gauge (which also assumes Weyl gauge $A_0^a = 0$). Implementing the Coulomb gauge by the Faddeev-Popov method, the expectation value of a functional $K[A]$ of the (spatial components of the) gauge field A is given by

$$\langle K[A] \rangle = \int_{\Omega} \mathcal{D}A \mathcal{J}[A] |\psi[A]|^2 K[A], \quad (8)$$

Here, $\psi[A] = \langle A | \psi \rangle$ denotes the Yang-Mills vacuum wave functional restricted to transverse fields, $\partial_i A_i^a = 0$, and $\mathcal{J}[A] = \text{Det}(G_A^{-1})$ is the Faddeev-Popov determinant with

$$G_A^{-1} = (-\delta^{ab} \partial_{\mathbf{x}}^2 - g \hat{A}_i^{ab}(\mathbf{x}) \partial_i^{\mathbf{x}}) \delta(\mathbf{x} - \mathbf{y}) \quad (9)$$

being the Faddeev-Popov operator. Since we work only with spatial vectors, we will use only Lorentz subscripts. Furthermore, g is the coupling constant, $\hat{A}^{ab} = f^{acb} A^c$ is the gauge field in the adjoint representation of the color group, and f^{acb} are the structure constants of the $\mathfrak{su}(N_c)$ algebra. The functional integration in Eq. (8) runs over transverse field configurations and is restricted to the first Gribov region Ω or, more precisely, to the fundamental modular region [23]. Moreover, we assume that the wave functional $\psi[A]$ is properly normalized: $\langle \psi | \psi \rangle \equiv \langle 1 \rangle = 1$. Writing the vacuum wave functional as in Eq. (3)

$$|\psi[A]|^2 = e^{-S[A]} \quad (10)$$

and choosing

$$K[A] = e^{\int j \cdot A}, \quad (11)$$

Eq. (8) becomes the generating functional of the static Green functions of the (transverse) gauge field A . In the following, it will be convenient not to fix $K[A]$ to the form (11) but rather to let $K[A]$ be an arbitrary functional of the gauge field. Furthermore, to simplify the bookkeeping we will use the compact notation

$$A_{k_1}^{a_1}(\mathbf{x}_1) = A(1),$$

$$A \cdot B = A(1)B(1) = \int d^d x A_i^a(\mathbf{x}) B_i^a(\mathbf{x}), \quad (12)$$

such that a repeated label means summation over the discrete color and Lorentz indices along with integration over the spatial coordinates.

Consider now the following identity:

$$0 = \int_{\Omega} \mathcal{D}A \frac{\delta}{\delta A(1)} \{ \mathcal{J}[A] e^{-S[A]} K[A] \}, \quad (13)$$

which holds due to the fact that the Faddeev-Popov determinant $\mathcal{J}[A]$ vanishes on the Gribov horizon $\partial\Omega$, tacitly assuming that the considered functional $K[A]$ does not spoil the vanishing of $\mathcal{J}[A]K[A]$ on $\partial\Omega$. Equation (13) with $K[A]$ given by Eq. (11) becomes the ordinary DSE of the usual (Lagrangian-based) functional integral formulation of Yang-Mills theory in Coulomb gauge [24] when the functional integration is extended over time-dependent gauge fields $A_{\mu}(\mathbf{x}, t)$ and $S[A]$ is chosen as the usual classical action of Yang-Mills theory.

Working out the functional derivative in Eq. (13) yields the following identity:

$$\left\langle \left[\frac{\delta \ln \mathcal{J}}{\delta A(1)} - \frac{\delta S[A]}{\delta A(1)} \right] K[A] \right\rangle + \left\langle \frac{\delta K[A]}{\delta A(1)} \right\rangle = 0. \quad (14)$$

The derivative of $\ln \mathcal{J}$ can be written as

$$\frac{\delta \ln \mathcal{J}}{\delta A(1)} = \frac{\delta}{\delta A(1)} \text{Tr} \ln G_A^{-1} = \tilde{\Gamma}_0(1; 3, 2) G_A(2, 3), \quad (15)$$

where we have introduced the bare ghost-gluon vertex²

$$\tilde{\Gamma}_0(1; 2, 3) = \frac{\delta G_A^{-1}(2, 3)}{\delta A(1)}. \quad (16)$$

With this result, Eq. (14) can be cast in the form

$$\left\langle \frac{\delta S[A]}{\delta A(1)} K[A] \right\rangle = \left\langle \frac{\delta K[A]}{\delta A(1)} \right\rangle + \tilde{\Gamma}_0(1; 3, 2) \langle G_A(2, 3) K[A] \rangle, \quad (17)$$

which is the basis of the gluon DSEs, exploited below in the evaluation of $\langle H \rangle$.

Introducing ghost fields in the usual way

$$\mathcal{J}[A] = \text{Det}(G_A^{-1}) = \int \mathcal{D}\bar{c} \mathcal{D}c e^{-\bar{c} G_A^{-1} c}, \quad (18)$$

the expectation value (8) explicitly reads

$$\langle K[A] \rangle = \int_{\Omega} \mathcal{D}A \int \mathcal{D}\bar{c} \mathcal{D}c K[A] e^{-S[A] - \bar{c} G_A^{-1} c}, \quad (19)$$

and Eq. (17) can be written as

$$\left\langle \frac{\delta S[A]}{\delta A(1)} K[A] \right\rangle = \left\langle \frac{\delta K[A]}{\delta A(1)} \right\rangle + \tilde{\Gamma}_0(1; 3, 2) \langle c(2) \bar{c}(3) K[A] \rangle. \quad (20)$$

The bare vertex $\tilde{\Gamma}_0$ is the lowest-order perturbative contribution [7] to the full ghost-gluon vertex $\tilde{\Gamma}$ defined by

$$\begin{aligned} \langle A(1) G_A(2, 3) \rangle &= \langle A(1) c(2) \bar{c}(3) \rangle \\ &= -D(1, 1') G(2, 2') \tilde{\Gamma}(1'; 2', 3') G(3', 3), \end{aligned} \quad (21)$$

where

$$D(1, 2) = \langle A(1) A(2) \rangle \quad (22)$$

is the gluon propagator and

$$G(1, 2) := \langle G_A(1, 2) \rangle = \langle c(1) \bar{c}(2) \rangle \quad (23)$$

is the ghost propagator.

Equation (20) [or equivalently Eq. (17)] is the basic DSE of the Hamiltonian formulation of Yang-Mills theory in Coulomb gauge, and we will refer to it as the ‘‘Hamiltonian DSE.’’ Below, we will exploit this equation to express the various static (equal-time) correlators occurring in the vacuum expectation value of the Hamilton operator by the variational kernels γ_n [Eq. (5)] of the wave functional $\psi[A]$. This requires appropriate choices of the so far arbitrary functional $K[A]$.

III. EXPRESSING STATIC CORRELATORS THROUGH PROPAGATORS AND PROPER VERTEX FUNCTIONS

Choosing the functional $K[A]$ in Eq. (20) as

$$K[A] = \exp\{j \cdot A + \bar{c} \cdot \eta + \bar{\eta} \cdot c\}, \quad (24)$$

where j and $\bar{\eta}, \eta$ are the gluon and ghost sources, respectively, we obtain the generating functional of the full static (equal-time) Green functions

$$Z[j, \eta, \bar{\eta}] = \langle \exp\{jA + \bar{c}\eta + \bar{\eta}c\} \rangle =: e^{W[j, \eta, \bar{\eta}]}, \quad (25)$$

where $W[j, \bar{\eta}, \eta]$ is the generating functional of the connected Green functions

$$\begin{aligned} \left. \frac{\delta W}{\delta j(1)} \right|_{j=\bar{\eta}=\eta=0} &= \langle A(1) \rangle = 0, \\ \left. \frac{\delta^2 W}{\delta j(1) \delta j(2)} \right|_{j=\bar{\eta}=\eta=0} &= \langle A(1) A(2) \rangle, \\ \left. \frac{\delta^3 W}{\delta j(1) \delta \bar{\eta}(2) \delta \eta(3)} \right|_{j=\bar{\eta}=\eta=0} &= -\langle A(1) c(2) \bar{c}(3) \rangle, \text{ etc.} \end{aligned} \quad (26)$$

Introducing the classical fields as³

$$A = \frac{\delta W}{\delta j}, \quad \bar{c} = -\frac{\delta W}{\delta \eta}, \quad c = \frac{\delta W}{\delta \bar{\eta}}, \quad (27)$$

we can define the effective action $\Gamma[A, \bar{c}, c]$ through the Legendre transform

$$\Gamma[A, \bar{c}, c] + W[j, \eta, \bar{\eta}] = j \cdot A + \bar{c} \cdot \eta + \bar{\eta} \cdot c, \quad (28)$$

where the sources have to be expressed by Eqs. (27) in terms of the classical fields A, \bar{c} , and c . From the effective action Eq. (28), the sources are obtained as

$$j = \frac{\delta \Gamma}{\delta A}, \quad \eta = \frac{\delta \Gamma}{\delta \bar{c}}, \quad \bar{\eta} = -\frac{\delta \Gamma}{\delta c}. \quad (29)$$

Using Eqs. (27), differentiation with respect to the gluonic source can be expressed as

$$\begin{aligned} \frac{\delta}{\delta j(1)} &= \frac{\delta A(2)}{\delta j(1)} \frac{\delta}{\delta A(2)} + \frac{\delta c(2)}{\delta j(1)} \frac{\delta}{\delta c(2)} + \frac{\delta \bar{c}(2)}{\delta j(1)} \frac{\delta}{\delta \bar{c}(2)} \\ &= \frac{\delta^2 W}{\delta j(1) \delta j(2)} \frac{\delta}{\delta A(2)} + \frac{\delta^2 W}{\delta j(1) \delta \bar{\eta}(2)} \frac{\delta}{\delta c(2)} \\ &\quad - \frac{\delta^2 W}{\delta j(1) \delta \eta(2)} \frac{\delta}{\delta \bar{c}(2)}. \end{aligned} \quad (30)$$

Similar expressions can be written for the derivatives with respect to the ghost sources. Differentiating Eqs. (29) and

²The bare ghost-gluon vertex $\tilde{\Gamma}_0$ defined by Eq. (16) differs from the one of Ref. [4] by an overall sign.

³With a slight abuse of notation, we employ the same symbol for both the classical fields and the quantum fields which are integrated over. No confusion should arise, since they never appear together. Furthermore, derivatives with respect to Grassmann fields are always left derivatives.

using Eqs. (27) and (30), we can link, in the usual way, the connected Green functions (derivatives of W) with the proper vertex functions (derivatives of Γ). As an example, we explicitly show how to express the full ghost-gluon vertex $\tilde{\Gamma}(1; 2, 3)$, defined in Eq. (21), by derivatives of the effective action. We start from the identity

$$\begin{aligned} \delta(1, 2) &= \frac{\delta}{\delta\eta(1)} \frac{\delta\Gamma}{\delta\bar{c}(2)} \\ &= \frac{\delta^2 W}{\delta\eta(1)\delta j(2')} \frac{\delta^2\Gamma}{\delta A(2')\delta\bar{c}(2)} + \frac{\delta^2 W}{\delta\eta(1)\delta\bar{\eta}(2')} \\ &\quad \times \frac{\delta^2\Gamma}{\delta c(2')\delta\bar{c}(2)} - \frac{\delta^2 W}{\delta\eta(1)\delta\eta(2')} \frac{\delta^2\Gamma}{\delta\bar{c}(2')\delta\bar{c}(2)}, \end{aligned} \quad (31)$$

which can be derived along the line of Eq. (30). Differentiating Eq. (31) with respect to a gluonic source $j(3)$ and using Eq. (30) yields

$$\begin{aligned} 0 &= \frac{\delta^3 W}{\delta j(3)\delta\eta(1)\delta\bar{\eta}(2')} \frac{\delta^2\Gamma}{\delta c(2')\delta\bar{c}(2)} + \frac{\delta^2 W}{\delta\eta(1)\delta\bar{\eta}(2')} \\ &\quad \times \frac{\delta^2 W}{\delta j(3)\delta j(3')} \frac{\delta^3\Gamma}{\delta A(3')\delta c(2')\delta\bar{c}(2)} + \dots, \end{aligned} \quad (32)$$

where the omitted terms vanish when the sources are set to zero. By means of Eq. (26) and of

$$\left. \frac{\delta^2\Gamma[A, \bar{c}, c]}{\delta c(2)\delta\bar{c}(1)} \right|_{A=\bar{c}=c=0} = G^{-1}(1, 2), \quad (33)$$

$$\begin{aligned} \langle A(1)A(2)A(3)A(4) \rangle &= D(1, 2)D(3, 4) + D(1, 3)D(2, 4) + D(1, 4)D(2, 3) + D(1', 1)D(2', 2)D(3', 3)D(4', 4) \\ &\quad \{-\Gamma(1', 2', 3', 4') \\ &\quad + D(5, 5')[\Gamma(1', 2', 5)\Gamma(5', 3', 4') + \Gamma(1', 3', 5)\Gamma(5', 2', 4') + \Gamma(1', 4', 5)\Gamma(5', 2', 3')]\}, \end{aligned} \quad (39)$$

$$\begin{aligned} \langle A(1)A(2)A(3)A(4)A(5) \rangle &= -\Gamma(1', \dots, 5')D(1, 1') \dots D(5, 5') + [\langle A(1)A(2)A(6) \rangle \Gamma(6, 3', 4', 5')D(3, 3')D(4, 4')D(5, 5') \\ &\quad + 9 \text{ combinations}] - [D(1, 1')\langle A(1')A(6)A(7) \rangle \Gamma(6, 6')\Gamma(7, 7')\langle A(6')A(2)A(3) \rangle \langle A(7')A(4)A(5) \rangle \\ &\quad + 14 \text{ combinations}] - [D(1, 2)\langle A(3)A(4)A(5) \rangle + 9 \text{ combinations}]. \end{aligned} \quad (40)$$

The proper n -point gluonic functions $\Gamma(1, 2, \dots, n)$ (36) are by definition invariant with respect to a permutation of external legs, i.e., of the entries $1, 2, \dots, n$. Equations (38)–(40) are represented in diagrammatic form in Figs. 1–3. The prefactors in Figs. 2 and 3 indicate the number of the



FIG. 1. Expression of the gluon three-point function [Eq. (38)] by means of three-point proper vertex function and propagators. Here and in the following, fat shaded gray blobs represent full Green's functions, small filled dots connected Green's functions, and small empty dots proper vertex functions.

the last relation can be expressed as

$$\begin{aligned} 0 &= -G^{-1}(2, 2')\langle A(3)\bar{c}(1)c(2') \rangle + G(2', 1)D(3, 3') \\ &\quad \times \left. \frac{\delta^3\Gamma[A, \bar{c}, c]}{\delta c(2')\delta\bar{c}(2)\delta A(3')} \right|_{A=\bar{c}=c=0}. \end{aligned} \quad (34)$$

Comparison with Eq. (21) shows

$$\tilde{\Gamma}(1; 2, 3) = \left. \frac{\delta^3\Gamma[A, \bar{c}, c]}{\delta c(3)\delta\bar{c}(2)\delta A(1)} \right|_{A=\bar{c}=c=0}. \quad (35)$$

Similarly, defining the n -gluon proper vertex function by

$$\Gamma_n \equiv \Gamma(1, 2, \dots, n) = \left. \frac{\delta^n\Gamma[A, \bar{c}, c]}{\delta A(1)\delta A(2)\dots\delta A(n)} \right|_{A=\bar{c}=c=0}, \quad (36)$$

the full gluon $n = 2, 3, 4, 5$ -point functions defined by Eq. (8) with $K[A] = AA\dots$ can be expressed through the proper vertex functions as

$$D(1, 2) \equiv \langle A(1)A(2) \rangle = \Gamma(1, 2)^{-1}, \quad (37)$$

$$\langle A(1)A(2)A(3) \rangle = -\Gamma(1', 2', 3')D(1', 1)D(2', 2)D(3', 3), \quad (38)$$

possible combinations. Consider, e.g., the second diagram on the right-hand side of Fig. 3: Out of the five external legs one can form $\binom{5}{2} = 10$ pairs of external legs attached to the right vertex. The remaining three external legs have to be attached then to the left vertex and thus do not add more possible combinations. In the third diagram there are five possibilities to select the external leg attached to the internal lines. From the remaining 4 external legs there are

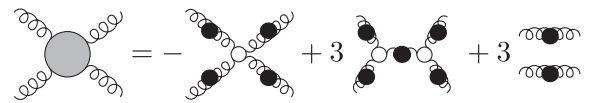


FIG. 2. Expression of the full gluon four-point function [Eq. (39)]. The prefactors indicate the number of possible permutations.

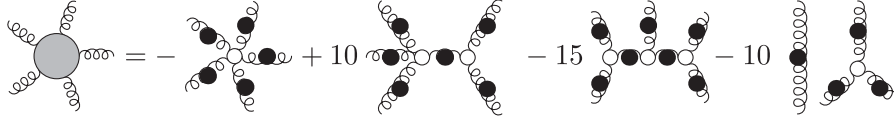


FIG. 3. Expression for the full gluon five-point Green function [Eq. (40)].

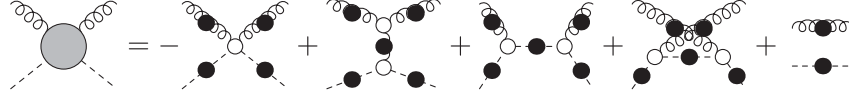


FIG. 4. Vacuum expectation value of two gauge fields and a ghost and an antighost field after Eq. (41).

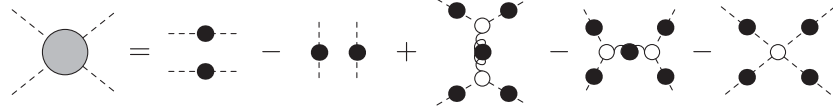


FIG. 5. Vacuum expectation value of two ghost and two antighost fields [Eq. (44)].

$\binom{4}{2} = 6$ possibilities to choose the two external legs at the right external vertex. This fixes also the external legs at the left vertex. The symmetry of the diagram with respect to the interchange of the two external vertices introduces an extra

factor $\frac{1}{2}$. Therefore this diagram occurs with the multiplicity $5 \cdot 6 \cdot \frac{1}{2} = 15$.

In a similar fashion one finds for the expectation value of two gauge fields and a ghost and antighost field

$$\langle A(1)A(2)c(3)\bar{c}(4) \rangle = \langle A(1)A(2)G_A(3,4) \rangle$$

$$= D(1,2)G(3,4) + D(1',1)D(2',2)G(3,3')G(4',4)\{-\tilde{\Gamma}(1',2';3',4') + \Gamma(1',2',5)D(5,5')\tilde{\Gamma}(5';3',4') + \tilde{\Gamma}(1';3',5)G(5,5')\tilde{\Gamma}(2';5',4') + \tilde{\Gamma}(2';3',5)G(5,5')\tilde{\Gamma}(1';5',4')\}, \quad (41)$$

where the two-gluon–two-ghost vertex is defined by

$$\tilde{\Gamma}(1,2;3,4) = \frac{\delta^4 \Gamma[A, \bar{c}, c]}{\delta c(4)\delta \bar{c}(3)\delta A(2)\delta A(1)} \Big|_{A=\bar{c}=c=0}. \quad (42)$$

The diagrammatic representation of Eq. (41) is shown in Fig. 4.

The last four-point function we need for the evaluation of $\langle H \rangle$ is the ghost four-point function

$$\langle c(1)\bar{c}(2)c(3)\bar{c}(4) \rangle = \langle [G_A(1,2)G_A(3,4) - G_A(1,4)G_A(3,2)] \rangle, \quad (43)$$

which can be expressed in terms of propagators and proper vertices in the standard way, yielding

$$\langle c(1)\bar{c}(2)c(3)\bar{c}(4) \rangle = G(1,2)G(3,4) - G(1,4)G(3,2) + G(1,1')G(3,3')\tilde{\Gamma}(5;1',2')D(5,5')\tilde{\Gamma}(5';3',4')[G(2',2)G(4',4) - G(2',4)G(4',2)] - \tilde{\Gamma}(1',3',2',4')G(1,1')G(2',2)G(3,3')G(4',4), \quad (44)$$

where the four-ghost vertex is defined by

$$\tilde{\Gamma}(1,3,2,4) = \frac{\delta^4 \Gamma[A, \bar{c}, c]}{\delta c(4)\delta c(2)\delta \bar{c}(3)\delta \bar{c}(1)} \Big|_{A=\bar{c}=c=0}. \quad (45)$$

Equation (44) is represented diagrammatically in Fig. 5.

IV. THE VACUUM WAVE FUNCTIONAL AND CORRESPONDING DSES

So far, all manipulations have been exact. In Sec. II B we have presented the Hamiltonian DSEs for arbitrary

wave functionals. To proceed further, we have to make an ansatz for the form of the vacuum wave functional $\psi[A]$, which by Eq. (10) defines the action functional $S[A]$.

In perturbation theory, the vacuum wave functional in the form (3) and (5) has been determined up to order $\mathcal{O}(g^2)$ by a solution of the Schrödinger equation, and the resulting expressions for the kernels γ_2 , γ_3 , and γ_4 are given in Ref. [25]. In the present nonperturbative approach, we will assume a wave functional of the form (3) and (5), with an action functional to be given by

$$S[A] = \omega(1, 2)A(1)A(2) + \frac{1}{3!}\gamma(1, 2, 3)A(1)A(2)A(3) + \frac{1}{4!}\gamma(1, 2, 3, 4)A(1)A(2)A(3)A(4). \quad (46)$$

For historical reasons, we have denoted $\frac{1}{2}\gamma(1, 2)$ by $\omega(1, 2)$. Consistent with our convention on the proper vertices Eq. (36), we will frequently use the shorthand $\gamma_n \equiv \gamma(1, \dots, n)$. The functions $\omega \equiv \frac{1}{2}\gamma_2$, γ_3 , and γ_4 are variational kernels which will be determined by minimization of the vacuum energy density. As discussed before, Eq. (46) can be considered as arising in leading orders of a systematic Taylor expansion of the action functional.

Let us also stress that the ghost fields do not enter the Yang-Mills vacuum wave functional $\psi[A]$. The ghost fields are auxiliary fields to represent the Faddeev-Popov determinant in local action form. By the very definition of the ghost fields [Eq. (18)], the ghost-gluon vertex in the action [i.e., the exponent of Eq. (19)] has to be the bare vertex and, in principle, there is absolutely no need to include ghost or ghost-gluon kernels as variational kernels in the wave functional. However, due to approximations to be introduced, for practical purposes, one might also include ghost or ghost-gluon vertices as variational kernels in the wave functional to improve the latter. If the exact gluon wave functional $\psi[A]$ were used, the variational principle would determine the ghost-gluon kernel as the bare one and higher ghost kernels to vanish. Therefore we will not include additional ghost vertices into the variational ansatz for the vacuum wave functional.

By construction, the variational kernels γ_n (which are purely gluonic) are totally symmetric with respect to permutations of the overall indices. Furthermore, the wave functional defined by Eqs. (10) and (46) is normalizable even when the restriction of the functional integration to the first Gribov region is ignored, provided the kernel γ_4 is positive definite, which we will assume for the moment and which later on will be confirmed by our calculations. With the action functional Eq. (46), the Hamiltonian DSE (17) becomes

$$2\omega(1, 2)\langle A(2)K[A] \rangle + \frac{1}{2}\gamma(1, 2, 3)\langle A(2)A(3)K[A] \rangle + \frac{1}{3!}\gamma(1, 2, 3, 4)\langle A(2)A(3)A(4)K[A] \rangle = \left\langle \frac{\delta K[A]}{\delta A(1)} \right\rangle + \tilde{\Gamma}_0(1; 3, 2)\langle G_A(2, 3)K[A] \rangle. \quad (47)$$

Except for the nonlocality of the variational kernels ω , γ_3 , and γ_4 , the functional Eq. (46) has the same structure as the ordinary Yang-Mills action. Therefore, the DSEs resulting from Eq. (47) will have the same structure as the DSEs of ordinary $d = 3$ Yang-Mills theory in Landau gauge, however with bare vertices replaced by the nonlocal variational kernels ω , γ_3 , and γ_4 . Equation (47) is our fundamental

DSE for the Hamiltonian approach to Yang-Mills theory in Coulomb gauge.

A. DSEs of gluonic vertex functions

The first DSE is obtained by setting $K[A] = 1$ in Eq. (47). Using $\langle A \rangle = 0$ and the expression Eq. (38) for the three-point function yields the identity

$$0 = \frac{1}{2}\gamma(1, 2, 3)D(2, 3) - \tilde{\Gamma}_0(1; 3, 2)G(2, 3) - \frac{1}{3!}\gamma(1, 2, 3, 4)\Gamma(2', 3', 4')D(2, 2')D(3, 3')D(4, 4'), \quad (48)$$

which is diagrammatically illustrated in Fig. 6. Equation (48) is not really a dynamical equation but rather a constraint, which can be used to simplify tadpole terms in the evaluation of higher-order DSEs. It is also easy to see that in lowest-order perturbation theory each term in Eq. (48) vanishes separately.

The DSE for the gluon propagator follows from (47) by putting $K[A] = A$, yielding

$$2\omega(1, 3)\langle A(3)A(2) \rangle + \frac{1}{2}\gamma(1, 3, 4)\langle A(3)A(4)A(2) \rangle + \frac{1}{3!}\gamma(1, 3, 4, 5)\langle A(3)A(4)A(5)A(2) \rangle = t(1, 2) + \tilde{\Gamma}_0(1; 4, 3)\langle G_A(3, 4)A(2) \rangle, \quad (49)$$

where we have introduced the abbreviation

$$t(1, 2) \equiv \delta^{a_1 a_2} t_{k_1 k_2}(\mathbf{x}_1) \delta(\mathbf{x}_1 - \mathbf{x}_2) \quad (50)$$

and $t_{k_1 k_2}(\mathbf{x}_1) = \delta_{k_1 k_2} - \partial_{k_1}^{x_1} \partial_{k_2}^{x_1} / \partial_{x_1}^2$ is the transverse projector. By means of Eqs. (38) and (39), the three- and four-point functions in Eq. (49) can be expressed through the proper vertex functions Γ_n . By multiplying Eq. (49) by the inverse gluon propagator Eq. (37) and defining

$$D(1, 2)^{-1} = \Gamma(1, 2) =: 2\Omega(1, 2), \quad (51)$$

Eq. (49) can be cast in the form

$$\Omega(1, 2) = \omega(1, 2) - \xi(1, 2) + \chi(1, 2) + \phi_1(1, 2) - \phi_2(1, 2) + \phi_t(1, 2), \quad (52)$$

where we have introduced the following loop terms:

$$\frac{1}{2} \text{diagram} - \text{diagram} - \frac{1}{3!} \text{diagram} = 0$$

FIG. 6. Diagrammatic representation of Eq. (48). The empty square boxes denote the variational kernels γ_n .

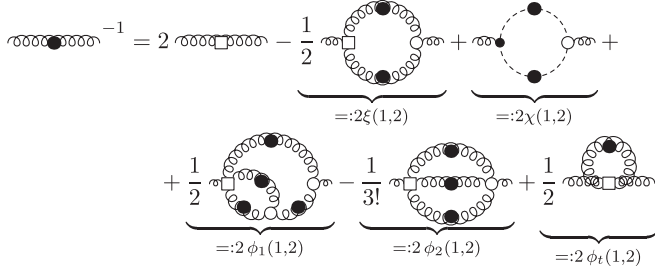


FIG. 7. Diagrammatic representation of the DSE for the gluon propagator [Eq. (52)].

$$\xi(1, 2) = \frac{1}{4}\gamma(1, 3, 4)D(3, 3')D(4, 4')\Gamma(3', 4', 2), \quad (53a)$$

$$\chi(1, 2) = \frac{1}{2}\tilde{\Gamma}_0(1; 3, 4)G(3', 3)G(4, 4')\tilde{\Gamma}(2; 4', 3'), \quad (53b)$$

$$\begin{aligned} \phi_1(1, 2) &= \frac{1}{4}\gamma(1, 3, 4, 5)D(3, 3')D(4, 4')D(5, 5') \\ &\quad \times D(6, 6')\Gamma(4', 5', 6)\Gamma(3', 6', 2), \end{aligned} \quad (53c)$$

$$\begin{aligned} \phi_2(1, 2) &= \frac{1}{3!2}\gamma(1, 3, 4, 5)D(3, 3')D(4, 4')D(5, 5') \\ &\quad \times \Gamma(3', 4', 5', 2), \end{aligned} \quad (53d)$$

$$\phi_t(1, 2) = \frac{1}{2}\gamma(1, 2, 3, 4)D(3, 4). \quad (53e)$$

Equation (52) is represented diagrammatically in Fig. 7 and is recognized as the usual DSE for the gluon propagator of Landau-gauge Yang-Mills theory [26], except for the replacement of the bare Yang-Mills vertices (defined by the Yang-Mills Lagrangian) by the variational kernels γ_n [defined by the ansatz (46) for the vacuum functional], which are represented by open square boxes; see Fig. 8.

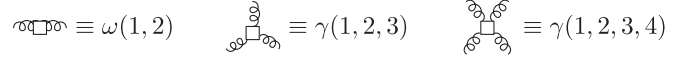


FIG. 8. Variational kernels occurring in the exponent of the wave functional.

Note that the gluon loop $\xi(1, 2)$ [Eq. (53a)] disappears when the three-gluon kernel γ_3 is absent from the exponential [Eq. (46)] of the wave functional [Eq. (10)]. For a Gaussian wave functional ($\gamma_3 = \gamma_4 = 0$) only the ghost loop $\chi(1, 2)$ [Eq. (53b)] survives from the loop terms in the DSE (52), Fig. 7.

Choosing $K[A] = A(2)A(3)$ in Eq. (47) yields the DSE for the three-gluon vertex,

$$\begin{aligned} 2\omega(1, 4)\langle A(4)A(2)A(3) \rangle &+ \frac{1}{2}\gamma(1, 4, 5)\langle A(4)A(5)A(2)A(3) \rangle \\ &+ \frac{1}{3!}\gamma(1, 4, 5, 6)\langle A(4)A(5)A(6)A(2)A(3) \rangle \\ &= \tilde{\Gamma}_0(1; 5, 4)\langle G_A(4, 5)A(2)A(3) \rangle. \end{aligned} \quad (54)$$

By means of Eqs. (38)–(41), the first two terms on the left-hand side and the right-hand side of Eq. (54) can be expressed in terms of proper vertex functions $\tilde{\Gamma}_n$. The explicit evaluation of the five-point function is quite lengthy, and we quote only the result. Restricting ourselves to terms involving up to one loop (which is sufficient to obtain the energy $\langle H \rangle$ up to three overlapping loops; see the introduction) and chopping off the external propagators, we eventually find from Eq. (54) the DSE for the proper three-point vertex function $\Gamma(1, 2, 3)$:

$$\begin{aligned} \Gamma(1, 2, 3) &= \gamma(1, 2, 3) + \gamma(1, 4, 5)D(4, 4')D(5, 5')D(6, 6')\Gamma(2, 4', 6)\Gamma(3, 5', 6') \\ &\quad - \tilde{\Gamma}_0(1; 4, 5)G(4', 4)G(5, 5')G(6', 6)[\tilde{\Gamma}(2; 6, 4')\tilde{\Gamma}(3; 5', 6') + 2 \leftrightarrow 3] \\ &\quad - \frac{1}{2}\gamma(1, 4, 5)D(4, 4')D(5, 5')\Gamma(4', 5', 2, 3) + \tilde{\Gamma}_0(1; 4, 5)G(4', 4)G(5, 5')\tilde{\Gamma}(2, 3; 5', 4') \\ &\quad - \frac{1}{2}[\gamma(1, 2, 4, 5)D(4, 4')D(5, 5')\Gamma(4', 5', 3) + 2 \leftrightarrow 3], \end{aligned} \quad (55)$$

which is represented diagrammatically in Fig. 9.

Analogously, one can derive the DSE for the four-gluon vertex. Restricting ourselves again up to three loops in the energy $\langle H \rangle$, one finds just the “tree-level” expression

$$\Gamma(1, 2, 3, 4) = \gamma(1, 2, 3, 4) + \dots, \quad (56)$$

which is represented diagrammatically in Fig. 10. Any loop contribution to Γ_4 generates at least four-loop terms in the energy, which are beyond the scope of the present paper.

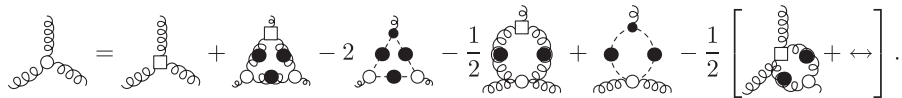


FIG. 9. Diagrammatic representation of the DSE (55) for the three-gluon proper vertex function. The factor of 2 in front of the ghost loop accounts for the two diagrams differing in the direction of the ghost line.

B. The DSEs for the ghost propagator and the ghost-gluon vertex

Inverting the defining equation of the Faddeev-Popov operator (9) one finds the following identity [4]:

$$G_A(1, 2) = G_0(1, 2) - G_A(1, 4)A(3)\tilde{\Gamma}_0(3; 4, 5)G_0(5, 2), \quad (57)$$

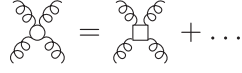


FIG. 10. Leading order DSE for the four-gluon vertex.



FIG. 11. Diagrammatic representation of the ghost DSE (58).

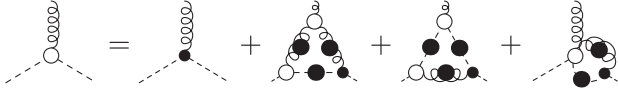


FIG. 12. Diagrammatic representation of the DSE (60) for the ghost-gluon vertex.

where $G_0(1, 2) = [(-\partial^2)^{-1}](1, 2)$ is the bare ghost propagator and $\tilde{\Gamma}_0$ is the bare ghost-gluon vertex defined in Eq. (16). Taking the expectation value of Eq. (57) and using Eq. (21) yields the usual DSE for the ghost propagator [4]:

$$G(1, 2)^{-1} = G_0(1, 2)^{-1} - \tilde{\Gamma}(3; 1, 4)G(4, 4')D(3, 3')\tilde{\Gamma}_0(3'; 4', 2), \quad (58)$$

which in momentum space reads

$$\begin{aligned} \tilde{\Gamma}(1; 2, 3) &= \tilde{\Gamma}_0(1; 2, 3) + \gamma(1, 4, 5)D(4, 4')D(5, 5')G(6, 6')\tilde{\Gamma}(4'; 2, 6)\tilde{\Gamma}(5'; 6', 3) \\ &+ \tilde{\Gamma}_0(1; 4, 5)G(4', 4)G(5, 5')D(6, 6')\tilde{\Gamma}(6, 2, 4')\tilde{\Gamma}(6'; 5', 3) - \frac{1}{2}\gamma(1, 4, 5)D(4, 4')D(5, 5')\tilde{\Gamma}(4', 5'; 2, 3) \\ &+ \tilde{\Gamma}(1; 4, 5)G(4', 4)G(5, 5')\tilde{\Gamma}(2, 5', 3, 4') \end{aligned} \quad (61)$$

and is shown in Fig. 13. The main difference between Eqs. (60) and (61) is that while Eq. (60) is exact, in Eq. (61) two-loops terms involving higher-order vertices are neglected. Nevertheless, to our purpose, calculating the energy up to three loops, Eq. (61) is more convenient. We will use this equation in Sec. V to simplify the expression for the kinetic and Coulomb energy.

V. ENERGY DENSITY OF THE YANG-MILLS VACUUM

The DSEs of the Hamiltonian approach derived in Sec. IV are not “equations of motion” in the usual sense but rather connect the various Green functions with the kernels occurring in the ansatz for the wave functional,



FIG. 13. Diagrammatic representation of the DSE (61) for the ghost-gluon vertex.

$$\begin{aligned} G^{-1}(\mathbf{p}) &= \mathbf{p}^2 + \frac{ig}{N_c^2 - 1} \int \frac{d^d q}{(2\pi)^d} f^{abc} \tilde{\Gamma}_i^{abc}(\mathbf{q}; \mathbf{p} - \mathbf{q}, \mathbf{p}) \\ &\times \frac{t_{ij}(\mathbf{p})q_j}{2\Omega(\mathbf{q})} G(\mathbf{p} - \mathbf{q}), \end{aligned} \quad (59)$$

and which is represented diagrammatically in Fig. 11.

To derive the DSE for the ghost-gluon vertex there are two possibilities. The first one is to multiply Eq. (57) by the gauge field and to take the expectation value of the resulting expression. This leads to

$$\langle A(1)G_A(2, 3) \rangle = -\langle A(1)A(4)G_A(2, 5) \rangle \tilde{\Gamma}_0(4; 5, 6)G_0(6, 3). \quad (60)$$

The remaining expectation value can be expressed in terms of proper vertices by means of Eqs. (21) and (41). After chopping off the external propagators, this results in the DSE for the ghost-gluon vertex shown in Fig. 12. Equation (60) is exact, i.e., not truncated, but not very convenient for the evaluation of the energy density. A more convenient form of the DSE for the ghost-gluon vertex is obtained by putting $K[A] = G_A$ in our general Hamiltonian DSE (47), thereby using the chain rule for the derivative of the ghost Green's function and using Eqs. (41) and (44) to express vacuum expectation values through propagators and proper vertex functions. The resulting equation reads at one-loop level

while these kernels themselves are at this point not yet fixed. Here is where the variational principle comes into play: We will now evaluate the expectation value of the Yang-Mills Hamiltonian for the wave functional (10) with the ansatz (46) and then minimize it with respect to the variational kernels γ_n .

The Yang-Mills Hamiltonian in Coulomb gauge reads [27]

$$\begin{aligned} H &= \int d^d x \left[\frac{1}{2} \mathcal{J}^{-1}[A] \Pi_i^a(\mathbf{x}) \mathcal{J}[A] \Pi_i^a(\mathbf{x}) + \frac{1}{4} F_{ij}^a(\mathbf{x}) F_{ij}^a(\mathbf{x}) \right] \\ &+ \frac{g^2}{2} \int d^d x d^d y \mathcal{J}^{-1}[A] \rho^a(\mathbf{x}) F_A^{ab}(\mathbf{x}, \mathbf{y}) \mathcal{J}[A] \rho^b(\mathbf{y}). \end{aligned} \quad (62)$$

Here, $\Pi_k^a(\mathbf{x}) = -i\delta/\delta A_k^a(\mathbf{x})$ is the momentum operator, and $F_{ij}^a = \partial_i A_j^a - \partial_j A_i^a + g f^{abc} A_i^b A_j^c$, is the non-Abelian field strength tensor. The first two terms in Eq. (62) are the electric (kinetic) and magnetic parts of the ordinary Yang-Mills Hamiltonian restricted to the curvilinear coordinate space of Coulomb gauge. The third (Coulomb) term arises from the resolution of Gauss's law and describes the interaction of the non-Abelian color charge (of the fluctuating gauge field) with density

$$\rho^a(\mathbf{x}) = \hat{A}_i^{ab}(\mathbf{x}) \Pi_i^b(\mathbf{x}) \quad (63)$$

through the non-Abelian Coulomb interaction kernel

$$F_A^{ab}(\mathbf{x}, \mathbf{y}) = [(-\hat{D}\partial)^{-1}(-\partial^2)(-\hat{D}\partial)^{-1}]_{\mathbf{x},\mathbf{y}}^{a,b}. \quad (64)$$

The Yang-Mills Hamiltonian in Coulomb gauge [Eq. (62)] is a positive definite operator. Accordingly the energy $\langle \psi | H | \psi \rangle$ is bounded from below (by zero) and the variational principle is applicable.

For later use, we rewrite the magnetic term of the Hamiltonian in the symmetrized form

$$\frac{1}{4} F_{ij}^a F_{ij}^a = -\frac{1}{2} A \partial^2 A + \frac{g}{3!} T_3 A^3 + \frac{g^2}{4!} T_4 A^4, \quad (65)$$

where the interaction kernels are given in momentum space by

$$T_{ijk}^{abc}(\mathbf{p}, \mathbf{q}, \mathbf{k}) = i f^{abc} [\delta_{ij}(p-q)_k + \delta_{jk}(q-k)_i + \delta_{ki}(k-p)_j] \quad (66a)$$

and

$$T_{ijkl}^{abcd} = \{ f^{abe} f^{cde} (\delta_{ik} \delta_{jl} - \delta_{il} \delta_{jk}) + f^{ace} f^{bde} (\delta_{ij} \delta_{kl} - \delta_{jk} \delta_{il}) + f^{ade} f^{bce} (\delta_{ij} \delta_{kl} - \delta_{ik} \delta_{jl}) \}. \quad (66b)$$

$$\left\langle \frac{\delta S[A]}{\delta A(1)} \frac{\delta S[A]}{\delta A(2)} f[A] \right\rangle = \left\langle \frac{\delta^2 S[A]}{\delta A(1) \delta A(2)} f[A] \right\rangle + \left\langle \frac{\delta^2 f[A]}{\delta A(1) \delta A(2)} \right\rangle + \tilde{\Gamma}_0(1; 4, 3) \left\langle \frac{\delta f[A]}{\delta A(2)} G_A(3, 4) \right\rangle + \tilde{\Gamma}_0(2; 4, 3) \left\langle \frac{\delta f[A]}{\delta A(1)} G_A(3, 4) \right\rangle + \tilde{\Gamma}_0(1; 4, 3) \tilde{\Gamma}_0(2; 6, 5) \langle f[A] [G_A(3, 4) G_A(5, 6) - G_A(3, 6) G_A(5, 4)] \rangle. \quad (69)$$

We stress that this is an exact identity, which holds for $f[A]$ being an arbitrary functional of the gauge field only, i.e., not containing the momentum operator. Furthermore, it will be sometimes convenient to express the last expectation value in terms of ghost fields:

$$\begin{aligned} & \langle f[A] [G_A(3, 4) G_A(5, 6) - G_A(3, 6) G_A(5, 4)] \rangle \\ &= \langle f[A] c(3) \bar{c}(4) c(5) \bar{c}(6) \rangle. \end{aligned} \quad (70)$$

B. Kinetic energy

After an integration by parts, the vacuum expectation value of the kinetic part of the Yang-Mills Hamiltonian [first term in Eq. (62)] can be expressed as

The bare four-gluon vertex [Eq. (66b)] is independent of the momenta.

A. Technicalities

To evaluate the vacuum expectation values of the kinetic term and of the Coulomb Hamiltonian, it is convenient to perform an integration by parts in the gauge field. This leads to expressions of the form

$$\left\langle \frac{\delta S[A]}{\delta A(1)} \frac{\delta S[A]}{\delta A(2)} f[A] \right\rangle, \quad (67)$$

where $f[A]$ is a functional of the gauge field which does not contain any momentum operator. In principle, we could now explicitly write down the variations of the action (46) and evaluate the expectation value (67). Then one would recognize that some terms can be combined and simplified by using the DSEs (52) and (55). Therefore, a more efficient way to evaluate the expectation value (67) is to use the Hamiltonian DSEs from the very beginning.

Putting $K[A] = \delta S/\delta A(2) f[A]$ in the general DSE (17) we obtain

$$\begin{aligned} \left\langle \frac{\delta S[A]}{\delta A(1)} \frac{\delta S[A]}{\delta A(2)} f[A] \right\rangle &= \left\langle \frac{\delta^2 S[A]}{\delta A(1) \delta A(2)} f[A] \right\rangle \\ &+ \left\langle \frac{\delta f[A]}{\delta A(1)} \frac{\delta S[A]}{\delta A(2)} \right\rangle \\ &+ \tilde{\Gamma}_0(1; 3, 4) \left\langle \frac{\delta S[A]}{\delta A(2)} G_A(4, 3) \right\rangle. \end{aligned} \quad (68)$$

The last two terms on the right-hand side of Eq. (68) can again be reexpressed through the DSEs (17), thereby putting $K[A] = \delta f[A]/\delta A$ and $K[A] = G_A$, respectively, and using the definition of the bare ghost-gluon vertex $\tilde{\Gamma}_0$ [Eq. (16)]. This results finally in the relation

$$E_k = \frac{1}{2} \int_{\Omega} \mathcal{D}A \mathcal{J}[A] \frac{\delta \psi[A]}{\delta A(1)} \frac{\delta \psi[A]}{\delta A(1)} = \frac{1}{8} \left\langle \frac{\delta S[A]}{\delta A(1)} \frac{\delta S[A]}{\delta A(1)} \right\rangle. \quad (71)$$

The last expectation value has precisely the form of Eq. (69) with $f[A] = 1$ and the two external indices contracted. The terms in Eq. (69) involving functional derivatives of $f[A]$ then vanish, and with the explicit form of the action (46) we find for the kinetic energy

$$E_k = \frac{1}{8} [2\omega(1, 1) + 2\phi_t(1, 1) + \tilde{\Gamma}_0(1; 4, 3) \tilde{\Gamma}_0(1; 6, 5) \times \langle c(3) \bar{c}(4) c(5) \bar{c}(6) \rangle]. \quad (72)$$

Here, ϕ_t is the gluon tadpole term occurring in the gluon DSE (52) and being defined by Eq. (53e). The ghost four-point function $\langle c\bar{c}c\bar{c} \rangle$ occurring in the last term can be expressed by means of Eq. (44) in terms of propagators and proper functions. Contracting Eq. (44) with the two bare ghost-gluon vertices as in Eq. (72), one obtains

$$\begin{aligned} & \tilde{\Gamma}_0(1; 4, 3)\tilde{\Gamma}_0(1; 6, 5)\langle c(3)\bar{c}(4)c(5)\bar{c}(6) \rangle \\ &= 4\chi(1, 3)D(3, 4)\chi(4, 1) - [\tilde{\Gamma}_0(1; 5', 6') \\ & \quad + \tilde{\Gamma}_0(1; 4, 3)\tilde{\Gamma}(7; 3', 6')\tilde{\Gamma}(7'; 5', 4')G(3, 3') \\ & \quad \times G(4', 4)D(7, 7') \\ & \quad + \tilde{\Gamma}_0(1; 4, 3)\tilde{\Gamma}(3', 5', 4', 6')G(3, 3')G(4', 4) \\ & \quad \times G(6', 6)G(5, 5')\tilde{\Gamma}_0(1; 6, 5), \end{aligned} \quad (73)$$

where $\chi(1, 2)$ is the ghost loop defined by Eq. (53b). The terms in the square brackets represent precisely the first, third, and fifth terms of the right-hand side of the truncated DSE (61) for the ghost-gluon vertex. Therefore we can use Eq. (61) to rewrite the terms in the bracket in Eq. (73) in a more compact form:

$$\begin{aligned} E_k &= \frac{1}{4}[\omega(1, 1) + \phi_t(1, 1) - \chi(1, 1) \\ & \quad + 2\chi(1, 2)D(2, 3)\chi(3, 1) + \eta_c(1, 1) - \eta_2(1, 1)], \end{aligned} \quad (74)$$

where we have introduced the abbreviations

$$\begin{aligned} 2\eta_c(1, 2) &= \tilde{\Gamma}_0(1; 3, 4)G(3', 3)G(4, 4')G(5, 5')\tilde{\Gamma}(6'; 5', 3') \\ & \quad \times \tilde{\Gamma}(7'; 4', 5)D(6, 6')D(7, 7')\gamma_3(6, 7, 2), \\ 2\eta_2(1, 2) &= \tilde{\Gamma}_0(1; 3, 4)G(3', 3)G(4, 4')\tilde{\Gamma}(5', 6'; 4', 3') \\ & \quad \times D(5, 5')D(6, 6')\gamma_3(5, 6, 2); \end{aligned} \quad (75)$$

see Fig. 14. Equation (74) can be slightly rewritten by using the gluon DSE (52) to eliminate the variational kernel ω (or, more precisely, the sum $\omega + \phi_t$) in favor of the inverse gluon propagator [Eq. (51)]. Assuming furthermore that the various loop terms Eqs. (53) are color diagonal, e.g.,

$$\xi_{ij}^{ab}(\mathbf{k}) = \delta^{ab}t_{ij}(\mathbf{k})\xi(\mathbf{k}), \text{ etc.}, \quad (76)$$

which is guaranteed by global color invariance, we can express the kinetic energy in momentum space as

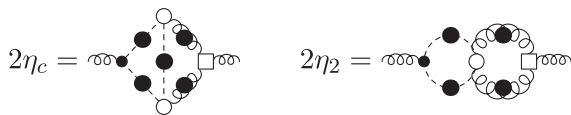


FIG. 14. Diagrammatic representation of the contributions (75) to the kinetic energy density.

$$\begin{aligned} E_k &= \frac{(N_c^2 - 1)(d - 1)}{4} V \int \tilde{d}p \left\{ \frac{[\Omega(\mathbf{p}) - \chi(\mathbf{p})]^2}{\Omega(\mathbf{p})} + \xi(\mathbf{p}) \right. \\ & \quad \left. - \phi_1(\mathbf{p}) + \phi_2(\mathbf{p}) - 2\eta_c(\mathbf{p}) \right\}, \end{aligned} \quad (77)$$

where the terms $\phi_{1,2}$ are defined in Eqs. (53c) and (53d), and η_c is given in Eq. (75). Furthermore, in Eq. (77) we have introduced the abbreviation

$$\tilde{d}p \equiv \frac{d^d p}{(2\pi)^d},$$

and V is the spatial volume which arises as in Ref. [4].

The ghost and gluon-loop contributions defined in Eqs. (53) read in momentum space

$$\begin{aligned} \chi(\mathbf{p}) &= \frac{t_{ij}(\mathbf{p})}{2(N_c^2 - 1)(d - 1)} \int \tilde{d}q \tilde{\Gamma}_{0,i}^{abc}(\mathbf{p}; \mathbf{q} - \mathbf{p}, -\mathbf{q}) \\ & \quad \times \tilde{\Gamma}_j^{acb}(-\mathbf{p}; \mathbf{q}, \mathbf{p} - \mathbf{q})G(\mathbf{q})G(\mathbf{p} - \mathbf{q}), \end{aligned} \quad (78)$$

$$\begin{aligned} \xi(\mathbf{p}) &= \frac{1}{16(N_c^2 - 1)(d - 1)} \\ & \quad \times \int \tilde{d}q d\mathbf{k} \frac{(\gamma_3 \circ \Gamma_3)(\mathbf{p}, \mathbf{q}, \mathbf{k})}{\Omega(\mathbf{q})\Omega(\mathbf{k})} \delta(\mathbf{p} + \mathbf{q} + \mathbf{k}). \end{aligned} \quad (79)$$

In the above equations, $\tilde{\Gamma}$ and Γ_3 are, respectively, the full ghost-gluon and three-gluon vertices defined by Eqs. (35) and (36). We have also introduced here the contraction of two color and Lorentz tensor structures through transverse projectors as

$$\begin{aligned} A \circ B &:= A_{ijk}^{abc}(\mathbf{p}, \mathbf{q}, \mathbf{k})t_{il}(\mathbf{p})t_{jm}(\mathbf{q})t_{kn}(\mathbf{k}) \\ & \quad \times B_{lmn}^{abc}(-\mathbf{p}, -\mathbf{q}, -\mathbf{k}). \end{aligned} \quad (80)$$

Furthermore, the term η_2 [Eq. (75)] has been discarded, since it gives rise exclusively to higher-order contributions with more than three loops in the energy, which are beyond our truncation scheme.

C. Magnetic energy

In the notation of Eq. (65) the magnetic energy is given by

$$E_B = \frac{1}{4}\langle F_{ij}^2 \rangle = -\frac{1}{2}\langle A\partial^2 A \rangle + \frac{g}{3!}T_3\langle A^3 \rangle + \frac{g^2}{4!}T_4\langle A^4 \rangle. \quad (81)$$

The first term on the right-hand side of Eq. (81) can be expressed by means of the gluon propagator (22), while the second term can be expressed through the proper three-point function Γ_3 [Eq. (38)]:

$$\frac{g}{3!}T_3\langle A^3 \rangle = -\frac{g}{3!}T_3 \circ \Gamma_3\langle AA \rangle^3. \quad (82)$$

In momentum space, these two energy contributions read

$$\frac{(N_c^2 - 1)(d - 1)}{4} V \int \tilde{d}p \frac{\mathbf{p}^2}{\Omega(\mathbf{p})} - \frac{gV}{8 \cdot 3!} \int \tilde{d}p \tilde{d}q dk \frac{(T_3 \circ \Gamma_3)(\mathbf{p}, \mathbf{q}, \mathbf{k})}{\Omega(\mathbf{p})\Omega(\mathbf{q})\Omega(\mathbf{k})} \delta(\mathbf{p} + \mathbf{q} + \mathbf{k}). \quad (83)$$

Let us turn now to the last term in Eq. (81), $\langle A^4 \rangle$. The four-point function is expressed by means of Eq. (39) in terms of gluon propagators and proper vertex functions. The disconnected terms in Eq. (39), i.e., the products of two gluon propagators, when contracted with the bare four-gluon vertex T_4 (66b) result in

$$g^2 \frac{N_c(N_c^2 - 1)}{16} V \int \tilde{d}p \tilde{d}q \frac{d(d - 3) + 3 - (\hat{\mathbf{p}} \cdot \hat{\mathbf{q}})^2}{\Omega(\mathbf{p})\Omega(\mathbf{q})}, \quad (84)$$

which is the usual gluon tadpole term, which occurs already when a Gaussian wave functional is used. Notice that, since the q integral does not depend on an external momentum, we can replace $\hat{q}_i \hat{q}_j \rightarrow \frac{1}{d} \delta_{ij}$ in the integrand, and using

$$d(d - 3) + 3 - \frac{1}{d} = \frac{(d - 1)^3}{d}$$

we can rewrite Eq. (84) as'

$$g^2 \frac{N_c(N_c^2 - 1)}{16} \frac{(d - 1)^3}{d} V \int \tilde{d}p \tilde{d}q \frac{1}{\Omega(\mathbf{p})\Omega(\mathbf{q})}. \quad (84)$$

Besides this, we get from the last term in Eq. (81) by using Eq. (39) also a contribution containing the proper four-point vertex function Γ_4 :

$$- \frac{g^2 V}{16 \cdot 4!} \int \tilde{d}p \tilde{d}q \tilde{d}k \tilde{d}\ell \frac{(T_4 \circ \Gamma_4)}{\Omega(\mathbf{p})\Omega(\mathbf{q})\Omega(\mathbf{k})\Omega(\ell)} \times \delta(\mathbf{p} + \mathbf{q} + \mathbf{k} + \ell), \quad (85)$$

and a contribution containing two three-gluon vertices

$$\frac{g^2 V}{8} \int \tilde{d}[pqk\ell] \times \frac{T_{ijmn}^{abcd} \Gamma_{ijl}^{abe}(-\mathbf{p}, -\mathbf{q}, \mathbf{p} + \mathbf{q}) \Gamma_{lmn}^{ecd}(\mathbf{k} + \ell, -\mathbf{k}, -\ell)}{32 \Omega(\mathbf{p})\Omega(\mathbf{q})\Omega(\mathbf{k})\Omega(\ell)\Omega(\mathbf{p} + \mathbf{q})} \times (2\pi)^d \delta(\mathbf{p} + \mathbf{q} + \mathbf{k} + \ell). \quad (86)$$

The Lorentz indices in Eq. (86) are supposed to be contracted by transverse projectors, which we have not explicitly written down in order to prevent the equation from getting cluttered. The various interaction contributions to the magnetic energy given by Eqs. (83)–(86) are shown in Fig. 15. Notice that the diagrams with a four-gluon vertex contain already three loops.

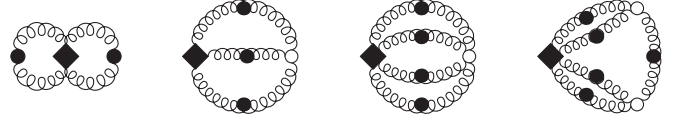


FIG. 15. Contributions from the three- and four-gluon vertices to the magnetic energy, from left to right: second term in Eqs. (83)–(86). The filled diamonds stand for the bare vertices T_3 and T_4 [Eqs. (66)] occurring in the magnetic part of the Hamilton operator [Eq. (65)].

D. Coulomb energy

After an integration by parts, as in the case of the kinetic energy, the vacuum expectation value of the Coulomb Hamiltonian, last term in Eq. (62), can be expressed as

$$E_c = \frac{g^2}{2} \int \mathcal{D}A \mathcal{J}[A] \int d^d x d^d y \left[\hat{A}_i^{ac}(\mathbf{x}) \frac{\delta \psi[A]}{i \delta A_i^c(\mathbf{x})} \right]^* \times F_A^{ab}(\mathbf{x}, \mathbf{y}) \left[\hat{A}_j^{bd}(\mathbf{y}) \frac{\delta \psi[A]}{i \delta A_j^d(\mathbf{y})} \right]. \quad (87)$$

In order to exploit our compact notation, we rewrite the color charge density (63) as

$$\rho(1) = R(1; 2, 3) A(2) \frac{\delta}{i \delta A(3)}, \quad (88)$$

where

$$R(1; 2, 3) = -R(1; 3, 2) = f^{a_1 a_2 a_3} \delta_{i_2 i_3} \delta(\mathbf{x}_1 - \mathbf{x}_2) \delta(\mathbf{x}_1 - \mathbf{x}_3). \quad (89)$$

In this notation, the Coulomb energy (87) reads

$$E_c = \frac{g^2}{8} R(1; 3, 4) R(2; 5, 6) \times \left\langle F_A(1, 2) A(3) A(5) \frac{\delta S[A]}{\delta A(4)} \frac{\delta S[A]}{\delta A(6)} \right\rangle. \quad (90)$$

The remaining expectation value can, in principle, be expressed in terms of (so far unknown) higher-order vertex functions. The required manipulations are, however, quite involved, and further simplifications are needed for practical reasons. Here we will again restrict ourselves to terms containing up to three overlapping loops in the energy. With this approximation we can factorize the Coulomb kernel F_A (see also Ref. [4]) as

$$E_c \simeq \frac{g^2}{8} R(1; 3, 4) R(2; 5, 6) \times \left\langle F_A(1, 2) \right\rangle \left\langle A(3) A(5) \frac{\delta S[A]}{\delta A(4)} \frac{\delta S[A]}{\delta A(6)} \right\rangle. \quad (91)$$

The Coulomb propagator $\langle F_A \rangle$ is discussed later in Sec. VIC. The remaining expectation value has precisely the form (67) with $f[A] = AA$, and from Eq. (69) we obtain

$$\begin{aligned}
\left\langle \frac{\delta S[A]}{\delta A(4)} \frac{\delta S[A]}{\delta A(6)} A(3)A(5) \right\rangle &= \left\langle \frac{\delta^2 S[A]}{\delta A(4)\delta A(6)} A(3)A(5) \right\rangle + \left\langle \frac{\delta^2}{\delta A(4)\delta A(6)} [A(3)A(5)] \right\rangle \\
&+ \tilde{\Gamma}_0(4; 8, 7) \left\langle \frac{\delta}{\delta A(6)} [A(3)A(5)] G_A(7, 8) \right\rangle + \tilde{\Gamma}_0(6; 8, 7) \left\langle \frac{\delta}{\delta A(4)} [A(3)A(5)] G_A(7, 8) \right\rangle \\
&+ \tilde{\Gamma}_0(4; 8, 7) \tilde{\Gamma}_0(6; 8', 7') \langle A(3)A(5) [G_A(7, 8)G_A(7', 8') - G_A(7, 8')G_A(7', 8)] \rangle. \quad (92)
\end{aligned}$$

When inserted into Eq. (91), this expression can be simplified by exploiting the color antisymmetry of the vertices R ; see Eq. (89): For this reason, the part of Eq. (92) symmetric with respect to the interchange of the indices ($3 \leftrightarrow 4$) or ($5 \leftrightarrow 6$) vanishes. Furthermore, the two terms on the right-hand side of Eq. (92) with a single (bare) ghost-gluon vertex $\tilde{\Gamma}_0$ yield identical contributions when inserted into Eq. (91).

The first four terms on the right-hand side of Eq. (92) can be straightforwardly evaluated as in the preceding sections. With the explicit form of the action (46), one obtains for these terms

$$\begin{aligned}
&t(3, 6)t(4, 5) + 2\tilde{\Gamma}_0(4; 8, 7)t(3, 6)\langle A(5)G_A(7, 8) \rangle \\
&+ 2\omega(4, 6)\langle A(3)A(5) \rangle + \gamma(4, 6, 7)\langle A(7)A(3)A(5) \rangle \\
&+ \frac{1}{2}\gamma(4, 6, 7, 8)\langle A(7)A(8)A(3)A(5) \rangle \\
&= t(3, 6)[t(4, 5) - 4\chi(4, 7)D(7, 5)] + 2\omega(4, 6)D(3, 5) \\
&- \gamma(4, 6, 7)D(5, 5')D(3, 3')D(5, 5')\Gamma(3', 5', 7') \\
&+ \frac{1}{2}\gamma(4, 6, 7, 8)\langle A(7)A(8)A(3)A(5) \rangle, \quad (93)
\end{aligned}$$

where we have used Eqs. (21) and (22), and the definition of the ghost loop [Eq. (53b)]. We are still left with the four-point function in Eq. (93) and with the six-point function in the last term in Eq. (92). To work out these terms, we notice that the Coulomb energy (91) can be diagrammatically represented as



where the ‘‘blob’’ (including the four lines attached to it) represents the vacuum expectation value given by the last bracket in Eq. (91) and the double line stands for the Coulomb propagator $\langle F_A \rangle$. Since we need the energy up to three loops, we should keep only those contributions to the blob which either factorize in two disconnected lines or are either irreducible or at most one-particle reducible (no box diagrams). At this order, for the last term in Eq. (93) it is sufficient to keep from the expression for $\langle A^4 \rangle$ given in Eq. (39) only the disconnected terms, yielding

$$\begin{aligned}
&\frac{1}{2}\gamma(4, 6, 7, 8)\langle A(7)A(8)A(3)A(5) \rangle \\
&= \frac{1}{2}\gamma(4, 6, 7, 8)[D(3, 5)D(7, 8) + D(3, 7)D(5, 8) \\
&\quad + D(3, 8)D(5, 7) + \dots] \\
&= D(3, 5)2\phi_t(4, 6) + \gamma(4, 6, 7, 8)D(7, 3)D(8, 5) + \dots, \quad (94)
\end{aligned}$$

where we have used the definition of gluon tadpole ϕ_t (53e) and made use of the symmetry properties of the four-gluon kernel γ_4 . The dots in Eq. (94) stand for terms which give rise to energy contributions with more than three loops. Following the same line of reasoning, the last term in Eq. (92) can be transformed to

$$\begin{aligned}
&\tilde{\Gamma}_0(4; 8, 7)\tilde{\Gamma}_0(6; 8', 7')\langle A(3)A(5) [G_A(7, 8)G_A(7', 8') - G_A(7, 8')G_A(7', 8)] \rangle \\
&= \tilde{\Gamma}_0(4; 8, 7)\tilde{\Gamma}_0(6; 8', 7')\{D(3, 5)\langle [G_A(7, 8)G_A(7', 8') - G_A(7, 8')G_A(7', 8)] \rangle + \langle A(3)G_A(7', 8') \rangle \langle A(5)G_A(7, 8) \rangle + \dots\} \\
&= D(3, 5)[-2\chi(4, 6) + 4\chi(4, 7)D(7, 8)\chi(8, 6) + \dots] + 4D(3, 7)\chi(7, 6)D(5, 8)\chi(8, 4) + \dots, \quad (95)
\end{aligned}$$

where we used Eqs. (21) and (44) and discarded terms involving more than three loops in the energy. Collecting all terms given by Eqs. (92)–(95) and inserting the result into (91), we finally obtain the Coulomb energy to the desired (three-loop) order:

$$\begin{aligned}
E_c &= \frac{g^2}{8}R(1; 3, 4)R(2; 5, 6)F(1, 2)\{2D(3, 5)[\omega(4, 6) + \phi_t(4, 6) - \chi(4, 6) + 2\chi(4, 7)D(7, 8)\chi(8, 6)] + t(3, 6)[t(4, 5) \\
&- 4\chi(4, 7)D(7, 5)] + 4D(3, 7)\chi(7, 6)D(5, 8)\chi(8, 4) - \gamma(4, 6, 7)D(5, 5')D(3, 3')D(5, 5')\Gamma(3', 5', 7') \\
&+ \gamma(4, 6, 7, 8)D(7, 3)D(8, 5)\}, \quad (96)
\end{aligned}$$

where $F(1, 2) = \langle F_A(1, 2) \rangle$. For later use we rewrite this expression in momentum space. Exploiting the symmetries of the entries and expressing the variational kernel ω through the inverse gluon propagator Ω , as we did for the kinetic energy, Eq. (96) can be cast into the form

$$\begin{aligned}
E_c = & g^2 \frac{N_c(N_c^2 - 1)}{16} V \int \tilde{d}p \tilde{d}q F(\mathbf{p} + \mathbf{q}) \frac{[d - 2 + (\hat{\mathbf{p}} \cdot \hat{\mathbf{q}})^2]}{\Omega(\mathbf{p})\Omega(\mathbf{q})} \{[\Omega(\mathbf{p}) - \chi(\mathbf{p}) - \Omega(\mathbf{q}) + \chi(\mathbf{q})]^2 + \xi(\mathbf{p})\Omega(\mathbf{p}) + \xi(\mathbf{q})\Omega(\mathbf{q})\} \\
& - V \frac{g^2}{8} \int \tilde{d}p \tilde{d}q \tilde{d}\ell F(\ell) \frac{t_{im}(\mathbf{p})t_{jn}(\mathbf{q})t_{kl}(\mathbf{p} + \mathbf{q})}{\Omega(\mathbf{p})\Omega(\mathbf{q})\Omega(\mathbf{p} + \mathbf{q})} f_{gad} f_{gbe} \gamma_{lmn}^{cde}(\mathbf{p} + \mathbf{q}, \ell - \mathbf{p}, -\mathbf{q} - \ell) \Gamma_{kij}^{cab}(-\mathbf{p} - \mathbf{q}, \mathbf{p}, \mathbf{q}) \\
& + V \frac{g^2}{8} \int \tilde{d}p \tilde{d}q \tilde{d}\ell F(\ell) \frac{t_{ij}(\mathbf{p})t_{lm}(\mathbf{q})}{\Omega(\mathbf{p})\Omega(\mathbf{q})} f^{abc} f^{ade} \gamma_{ilm}^{bdce}(\ell - \mathbf{p}, \mathbf{p}, -\ell - \mathbf{q}, \mathbf{q}), \tag{97}
\end{aligned}$$

where $F(\mathbf{k})$ is the Fourier representation of the Coulomb propagator $\langle F_A \rangle$; see Sec. VIC below. If we discard the three- and four-gluon kernels γ_3 and γ_4 , which also removes the gluon loop $\xi(\mathbf{p})$ [Eq. (53a)], this expression reduces to the Coulomb energy obtained in Refs. [4,5] with a Gaussian wave functional:

$$\begin{aligned}
E_c = & g^2 \frac{N_c(N_c^2 - 1)}{16} V \int \tilde{d}p \tilde{d}q F(\mathbf{p} + \mathbf{q}) \\
& \times \frac{[d - 2 + (\hat{\mathbf{p}} \cdot \hat{\mathbf{q}})^2]}{\Omega(\mathbf{p})\Omega(\mathbf{q})} [\Omega(\mathbf{p}) - \chi(\mathbf{p}) - \Omega(\mathbf{q}) + \chi(\mathbf{q})]^2. \tag{98}
\end{aligned}$$

The new features introduced by the inclusion of the three- and four-gluon kernels will be studied in the subsequent sections.

VI. DETERMINATION OF THE VARIATIONAL KERNELS

In the previous section we have expressed the vacuum energy $\langle \psi | H | \psi \rangle$ in terms of the variational kernels ω , γ_3 , and γ_4 [occurring in our ansatz (10) and (46) for the vacuum wave functional $\psi[A]$] and of the proper vertices Γ_n and $\tilde{\Gamma}_n$. We now use the DSEs (52), (55), (56), and (61) to express the proper vertex functions Γ_n and $\tilde{\Gamma}_n$ occurring in the energy in terms of the variational kernels γ_n . We are then in a position to determine these kernels by minimizing $\langle \psi | H | \psi \rangle$. To make the calculations feasible, we will resort to a skeleton expansion of $\langle \psi | H | \psi \rangle$, keeping at most three-loop terms. As we will see, this is the minimum number of loops required to obtain a nontrivial four-gluon kernel γ_4 . In the variation of the energy with respect to $\frac{1}{2}\gamma_2 = \omega$ and γ_3 we will restrict ourselves up to two-loop terms in $\langle \psi | H | \psi \rangle$, which will be sufficient to get a nontrivial γ_3 and a one-loop gap equation for ω .

A. Three- and four-gluon kernels

Below, we determine the three-gluon kernel in leading order in the number of loops. For this purpose, it is sufficient to keep up to two-loop terms in the energy. The relevant contributions come then from the gluon loop ξ (79) occurring in the kinetic energy (77) and the magnetic energy contribution (83). These terms contain the three-gluon kernel γ_3 either explicitly or implicitly via the three-point proper vertex Γ_3 , which by its DSE (55) is given in

lowest order by the three-gluon kernel γ_3 . All remaining terms of Γ_3 contain additional loops and will henceforth be discarded, resulting in the ‘‘tree-level’’ expression $\Gamma_3 = \gamma_3$. Inserting this expression in Eqs. (79) and (83) and taking into account the symmetry of these kernels, the variation of these energy terms with respect to the three-gluon kernel γ_3 leads to

$$\begin{aligned}
\frac{\delta}{\delta \gamma_3} \int \tilde{d}p \tilde{d}q \tilde{d}\ell \frac{\delta(\mathbf{p} + \mathbf{q} + \ell)}{\Omega(\mathbf{p})\Omega(\mathbf{q})\Omega(\ell)} \left[(\gamma_3 \circ \gamma_3) \right. \\
\left. \times \frac{\Omega(\mathbf{p}) + \Omega(\mathbf{q}) + \Omega(\ell)}{4} - (\gamma_3 \circ gT_3) \right] \stackrel{!}{=} 0, \tag{99}
\end{aligned}$$

which fixes the three-gluon kernel to

$$\gamma_{ijk}^{abc}(\mathbf{p}, \mathbf{q}, \mathbf{k}) = \frac{2gT_{ijk}^{abc}(\mathbf{p}, \mathbf{q}, \mathbf{k})}{\Omega(\mathbf{p}) + \Omega(\mathbf{q}) + \Omega(\mathbf{k})}, \tag{100}$$

where the tensor $T_{ijk}^{abc}(\mathbf{p}, \mathbf{q}, \mathbf{k})$ is defined in Eq. (66a). The obtained three-gluon kernel γ_3 is reminiscent of the perturbative one following from a solution of the Yang-Mills Schrödinger equation in leading order in the coupling constant g [25]:

$$\gamma_{ijk}^{(0)abc}(\mathbf{p}, \mathbf{q}, \mathbf{k}) = \frac{2gT_{ijk}^{abc}(\mathbf{p}, \mathbf{q}, \mathbf{k})}{|\mathbf{p}| + |\mathbf{q}| + |\mathbf{k}|}, \tag{101}$$

except that the perturbative gluon energy $|\mathbf{k}|$ is replaced in Eq. (100) by the nonperturbative one $\Omega(\mathbf{k})$. Note that, in principle, the Lorentz indices in Eqs. (100) and (101) are contracted with transverse projectors, which we did not explicitly write down, since they arise naturally as these kernels are always contracted with either transverse gauge fields or the corresponding transverse Green functions.

The variational determination of the four-gluon kernel γ_4 is technically somewhat more involved. The terms of $\langle H \rangle$ contributing to the variation with respect to γ_4 are those containing γ_4 either explicitly or implicitly via the DSEs (55) and (56) for the proper three- and four-gluon vertices Γ_3 and Γ_4 . Terms explicitly containing γ_4 are the $\phi_{1,2}$ terms Eqs. (53c) and (53d) of the kinetic energy Eq. (77), as well as the last term of the Coulomb energy (97). Terms containing Γ_3 or Γ_4 are given by the gluon loop ξ (79) in the kinetic energy (77) as well as by the magnetic energy contributions (83) and (85). All terms contributing to the variation of the energy with respect to γ_4 are collected below:

$$\begin{aligned}
& \frac{1}{4!2} \gamma(1, 2, 3, 4)D(1, 1')D(2, 2')D(3, 3')\gamma(1', 2', 3', 4) - \frac{1}{16} \gamma(1, 2, 3, 4)\gamma(3', 4', 5)D(5, 5')\gamma(5', 1, 2')D(2, 2')D(3, 3')D(4, 4') \\
& + \Gamma(1, 2, 3)D(1, 1')D(2, 2') \left[\frac{1}{16} \gamma(1', 2', 3) - \frac{1}{3!} D(3, 3')T(1', 2', 3') \right] \\
& - \frac{1}{4!} \gamma(1, 2, 3, 4)D(1, 1')D(2, 2')D(3, 3')D(4, 4')\gamma(1', 2', 3', 4') \\
& + \frac{g^2}{8} F(1, 2)R(1; 3, 4)R(2; 5, 6)\gamma(4, 6, 7, 8)D(7, 3)D(8, 5). \quad (102)
\end{aligned}$$

For simplicity, we have not explicitly symmetrized this expression with respect to a permutation of the indices of γ_4 .⁴ In the above expression we have used the DSE (56) to replace the four-gluon vertex Γ_4 by the four-gluon kernel γ_4 . To be consistent, we have to use the DSE for the three-gluon vertex [Eq. (55)] to express the vertex function Γ_3 in (102) by the variational kernels, where it is sufficient to retain only terms involving γ_4 or Γ_4 , and the latter is to be replaced by γ_4 due to the DSE (56). Taking into account the symmetry properties of the quantities involved, by

Eq. (55) we are led to make the following replacement in Eq. (102):

$$\begin{aligned}
\Gamma(1, 2, 3) & \rightarrow -\frac{1}{2}\gamma(3, 4, 5)D(4, 4')D(5, 5')\gamma(4', 5', 1, 2) \\
& - \gamma(3, 1, 4, 5)D(4, 4')D(5, 5')\gamma(4', 5', 2). \quad (103)
\end{aligned}$$

With this replacement, the variation of Eq. (102) with respect to γ_4 is now straightforward and yields after proper symmetrization with respect to external indices of γ_4

$$\begin{aligned}
& [\Omega(\mathbf{k}_1) + \Omega(\mathbf{k}_2) + \Omega(\mathbf{k}_3) + \Omega(\mathbf{k}_4)]\gamma_{ijkl}^{abcd}(\mathbf{k}_1, \mathbf{k}_2, \mathbf{k}_3, \mathbf{k}_4) \\
& = 2g^2 T_{ijkl}^{abcd} - \frac{1}{2} \{ \gamma_{ijm}^{abe}(\mathbf{k}_1, \mathbf{k}_2, -\mathbf{k}_1 - \mathbf{k}_2) t_{mn}(\mathbf{k}_1 + \mathbf{k}_2) \gamma_{klm}^{cde}(\mathbf{k}_3, \mathbf{k}_4, \mathbf{k}_1 + \mathbf{k}_2) + \gamma_{ikm}^{ace}(\mathbf{k}_1, \mathbf{k}_3, -\mathbf{k}_1 - \mathbf{k}_3) \\
& \quad \times t_{mn}(\mathbf{k}_1 + \mathbf{k}_3) \gamma_{jln}^{bde}(\mathbf{k}_2, \mathbf{k}_4, \mathbf{k}_1 + \mathbf{k}_3) + \gamma_{ilm}^{ade}(\mathbf{k}_1, \mathbf{k}_4, -\mathbf{k}_1 - \mathbf{k}_4) t_{mn}(\mathbf{k}_1 + \mathbf{k}_4) \gamma_{jkn}^{bce}(\mathbf{k}_2, \mathbf{k}_3, \mathbf{k}_1 + \mathbf{k}_4) \} \\
& - 2g^2 \{ f^{abe} f^{cde} \delta_{ij} \delta_{kl} [\Omega(\mathbf{k}_1) - \Omega(\mathbf{k}_2)] F(\mathbf{k}_1 + \mathbf{k}_2) [\Omega(\mathbf{k}_3) - \Omega(\mathbf{k}_4)] + f^{ace} f^{bde} \delta_{ik} \delta_{jl} [\Omega(\mathbf{k}_1) - \Omega(\mathbf{k}_3)] \\
& \quad \times F(\mathbf{k}_1 + \mathbf{k}_3) [\Omega(\mathbf{k}_2) - \Omega(\mathbf{k}_4)] + f^{ade} f^{bce} \delta_{il} \delta_{jk} [\Omega(\mathbf{k}_1) - \Omega(\mathbf{k}_4)] F(\mathbf{k}_1 + \mathbf{k}_4) [\Omega(\mathbf{k}_2) - \Omega(\mathbf{k}_3)] \}. \quad (104)
\end{aligned}$$

$F(\mathbf{p})$ is again the Fourier representation of the Coulomb propagator $\langle F_A \rangle$. Equation (104) yields a four-gluon kernel γ_4 , which is reminiscent of the perturbative one [25] except that the perturbative propagators and vertices are replaced by the full ones.

B. Gap equation

Given the explicit form of the energy functional (77), (83)–(86), and (97), it is more convenient to use the DSE (52) for the gluon propagator to express the kernel $\omega(\mathbf{p})$ in terms of the gluon energy $\Omega(\mathbf{p})$ and vary the energy density with respect to $\Omega^{-1}(\mathbf{p})$. The vacuum energy is given by closed loop diagrams, and the variation with respect to the gluon propagator $\Omega^{-1}(\mathbf{p})$ reduces the number of loops by one. If the (gap) equation for $\Omega(\mathbf{p})$ is to be calculated up to one loop, it is sufficient to keep up to two loops in the energy. At this order, the energy density ε defined by $\langle H \rangle =: V(d-1)(N_c^2 - 1)\varepsilon$ is given by

$$\begin{aligned}
\varepsilon & = \frac{1}{4} \int \tilde{d}p \frac{\mathbf{p}^2 + [\Omega(\mathbf{p}) - \chi(\mathbf{p})]^2}{\Omega(\mathbf{p})} \\
& - \frac{g^2 N_c}{3!8(d-1)} \int \tilde{d}p \tilde{d}q \frac{1}{\Omega(\mathbf{p})\Omega(\mathbf{q})\Omega(\mathbf{p} + \mathbf{q})} \\
& \times \gamma_3 \circ \left[\frac{\Omega(\mathbf{p}) + \Omega(\mathbf{q}) + \Omega(\mathbf{p} + \mathbf{q})}{4} \gamma_3 - gT_3 \right] \\
& + \frac{g^2 N_c}{16(d-1)} \int \tilde{d}p \tilde{d}q [d-2 + (\hat{\mathbf{p}} \cdot \hat{\mathbf{q}})^2] F(\mathbf{p} + \mathbf{q}) \\
& \times \frac{[\Omega(\mathbf{p}) - \chi(\mathbf{p}) - \Omega(\mathbf{q}) + \chi(\mathbf{q})]^2}{\Omega(\mathbf{p})\Omega(\mathbf{q})}; \quad (105)
\end{aligned}$$

see Eqs. (77), (83), and (98). In Eq. (105) we have discarded the tadpole term [Eq. (84) or (84)] since it represents an irrelevant constant, which disappears after renormalization. Except for the gluon loop (second term), the energy density Eq. (105) was already obtained in Refs. [4,5], where a Gaussian wave functional multiplied by $\mathcal{J}^{-1/2}[A]$ was used. The gluon loop is lost when a Gaussian wave functional is used, for which Green's functions with an odd number of fields vanish.

In principle, in Eq. (105) the three-gluon kernel γ_3 (100) obtained from the variational principle $\delta\varepsilon/\delta\gamma_3 = 0$ depends on $\Omega(\mathbf{p})$. However, since the energy density ε (105)

⁴Recall that, by definition, γ_4 is totally symmetric with respect to a permutation of indices. Strictly speaking, one should first symmetrize Eq. (102) and then take the variation. However, the same result is more conveniently obtained by taking the variation of the unsymmetrized expression and symmetrizing afterwards.

with γ_3 given by Eq. (100) is already stationary with respect to variations of γ_3 , we can ignore the implicit $\Omega(\mathbf{p})$ dependence of ε via γ_3 . Variation of ε (105) with respect to $\Omega^{-1}(\mathbf{k})$ then yields the gap equation

$$\Omega(\mathbf{p})^2 = \mathbf{p}^2 + \chi(\mathbf{p})^2 - I_G(\mathbf{p}) + I_C(\mathbf{p}), \quad (106)$$

where $\chi(\mathbf{p})$ is the ghost loop (78),

$$I_G(\mathbf{p}) = \frac{1}{4(d-1)(N_c^2 - 1)} \int \frac{d^d q}{(2\pi)^d} \frac{1}{\Omega(\mathbf{p})\Omega(\mathbf{p} + \mathbf{q})} \times \gamma_3 \circ \left[gT_3 - \gamma_3 \frac{\Omega(\mathbf{p}) + \Omega(\mathbf{p} + \mathbf{q})}{4} \right] \quad (107a)$$

is the gluon-loop contribution, and

$$I_C(\mathbf{p}) = \frac{g^2 N_c}{2(d-1)} \int \frac{d^d q}{(2\pi)^d} [d-2 + (\hat{\mathbf{k}} \cdot \hat{\mathbf{q}})^2] F(\mathbf{p} + \mathbf{q}) \times \frac{[\Omega(\mathbf{q}) - \chi(\mathbf{q}) + \chi(\mathbf{p})]^2 - \Omega(\mathbf{p})^2}{\Omega(\mathbf{q})} \quad (107b)$$

arises from the Coulomb term. Except for the gluon loop $I_G(\mathbf{k})$, Eq. (106) is the gap equation found already in [4].

If we insert the expression derived above in leading order for the three-gluon kernel γ_3 [Eq. (100)] into the gluon-loop contribution [Eq. (107a)], this takes the form

$$I_G(\mathbf{p}) = \frac{g^2 N_c}{d-1} \int \frac{d^d q}{(2\pi)^d} \frac{2\Omega(\mathbf{p}) + \Omega(\mathbf{q}) + \Omega(\mathbf{p} + \mathbf{q})}{[\Omega(\mathbf{p}) + \Omega(\mathbf{q}) + \Omega(\mathbf{p} + \mathbf{q})]^2} \times \frac{\Sigma(\mathbf{p}, \mathbf{q})}{\Omega(\mathbf{q})\Omega(\mathbf{p} + \mathbf{q})}, \quad (108)$$

where the function Σ arises from the contraction of the Lorentz structure of two three-gluon vertices upon imposing momentum conservation

$$T_3 \circ T_3|_{\mathbf{k}=-\mathbf{p}-\mathbf{q}} =: 4N_c(N_c^2 - 1)\Sigma(\mathbf{p}, \mathbf{q}) \quad (109)$$

and is given explicitly by

$$\Sigma(\mathbf{p}, \mathbf{q}) = [1 - (\hat{\mathbf{p}} \cdot \hat{\mathbf{q}})^2] \left[(d-1)(\mathbf{p}^2 + \mathbf{q}^2) + \frac{(d-2)\mathbf{p}^2\mathbf{q}^2 + (\mathbf{p} \cdot \mathbf{q})^2}{(\mathbf{p} + \mathbf{q})^2} \right]. \quad (110)$$

To exhibit the UV behavior of the various loop terms, let us consider them in leading order in perturbation theory [7,25], where $F(\mathbf{p}) = 1/\mathbf{p}^2$ and $\chi(\mathbf{p}) = 0$. In this order we find with 3-momentum cutoff Λ for the divergent parts

$$I_G(\mathbf{p}) = \frac{g^2 N_c}{(4\pi)^2} \left[\frac{4}{3} \Lambda^2 + \frac{22}{15} \mathbf{p}^2 \ln \frac{\Lambda^2}{\mathbf{p}^2} \right], \quad (111a)$$

$$I_C(\mathbf{p}) = \frac{g^2 N_c}{(4\pi)^2} \left[\frac{4}{3} \Lambda^2 - \frac{8}{15} \mathbf{p}^2 \ln \frac{\Lambda^2}{\mathbf{p}^2} \right]. \quad (111b)$$

One observes that the quadratic divergence in Eq. (106) cancels, and the sum of the logarithmic ones is consistent with the result of Lagrangian-based perturbation theory in Coulomb gauge [24,28]

$$\frac{|\mathbf{p}|}{\Omega(\mathbf{p})} = 1 + \frac{1}{2\mathbf{p}^2} [I_G(\mathbf{p}) - I_C(\mathbf{p})] + \dots = 1 + \frac{g^2 N_c}{(4\pi)^{2-\varepsilon}} \left(\frac{1}{\varepsilon} - \ln \frac{\mathbf{p}^2}{\mu^2} \right) + \dots, \quad (112)$$

where we have used dimensional regularization with $d = 3 - 2\varepsilon$.

To estimate the size of the contribution of the gluon loop (107a) to the gap equation (106), we use the gluon energy Ω obtained with a Gaussian wave functional in Ref. [8] as input. For practical purposes, we fit the $\Omega(\mathbf{p})$ obtained in Ref. [8] to the formula

$$\Omega(\mathbf{p}) = \sqrt{\mathbf{p}^2 + \frac{m_A^4}{\mathbf{p}^2} + c^2}, \quad (113)$$

which yields $m_A^4 \simeq 0.36\sigma_c^2$, $c^2 \simeq 1.0\sigma_c$. The numerical results of Ref. [8] and the fit to Eq. (113) are shown in Fig. 16. The gluon loop (107a) is UV-divergent. In principle, the UV-divergent part is removed by the renormalization of the gap equation (106), which can be done analogously to Refs. [12,29]. We therefore calculate

$$\Omega_{\text{new}}(\mathbf{p})^2 = \Omega_{\text{old}}(\mathbf{p})^2 - (I_G(\mathbf{p})[\Omega_{\text{old}}] - I_G(\mathbf{p})_{\text{div}}), \quad (114)$$

where $I_G(\mathbf{p})_{\text{div}}$ is the (known) perturbative divergent part of the gluon loop, which has been subtracted, and Eq. (113) has been used for $\Omega_{\text{old}}(\mathbf{p})$. The (inverse) gluon propagator $\Omega_{\text{new}}(\mathbf{p})$ [Eq. (114)] is shown in Fig. 17 together with the one obtained previously [8] with a Gaussian wave functional $\Omega_{\text{old}}(\mathbf{p})$. The mismatch in the UV is due to the anomalous dimension developed by $\Omega_{\text{new}}(\mathbf{p})$ and absent in $\Omega_{\text{old}}(\mathbf{p})$. As seen in Fig. 17, significant correction from the gluon loop arises in the midmomentum regime, a behavior which was observed also in Landau gauge [30,31]. This *a posteriori* supports the use of the Gaussian wave functional for the description of the infrared regime.

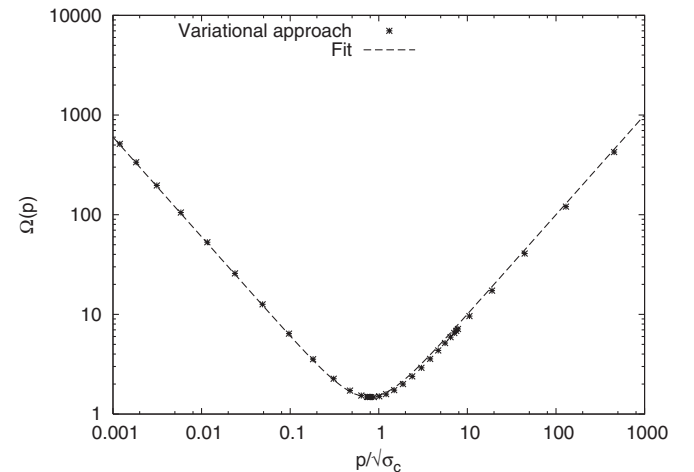


FIG. 16. Numerical results from Ref. [8] for the gluon energy $\Omega(\mathbf{p})$ and fit to Eq. (107a).

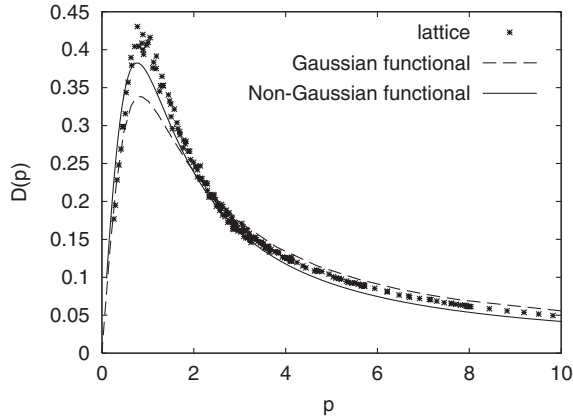


FIG. 17. Comparison of the gluon propagator obtained in Ref. [8] with a Gaussian wave functional (dashed line) with the corrected one from Eq. (114) (full line), and the lattice data from Ref. [9].

C. The Coulomb form factor

With the explicit expression of the three- and four-gluon kernels γ_3 [Eq. (100)] and γ_4 [Eq. (104)], on hand, we are left with three coupled equations: Eq. (59) for the ghost propagator, Eq. (61) for the ghost-gluon vertex, and the gap equation (106) for the gluon propagator. The final piece which is missing for closing this set of equations is the non-Abelian color Coulomb potential $F(1,2)$ defined by the vacuum expectation value of the Coulomb kernel [Eq. (64)]:

$$F(1,4) = \langle F_A(1,4) \rangle = \langle G_A(1,2)G_0^{-1}(2,3)G_A(3,4) \rangle. \quad (115)$$

The quantity $g^2 F(1,2)$ directly relates to the heavy quark potential [32] and is hence a renormalization group invariant quantity. Before we come to the evaluation of $\langle F_A \rangle$, let us remark that in practical application it is not necessary to explicitly solve the DSE (61) for the ghost-gluon vertex. Rather it is sufficient to replace the full ghost-gluon vertex $\tilde{\Gamma}$ [Eq. (35)] by the bare one $\tilde{\Gamma}_0$ [Eq. (16)]. This approximation is motivated by the “nonrenormalization” theorem for this vertex [33]. Although this theorem was originally proven [33] and confirmed on the lattice [34,35] for QCD in Landau gauge, the arguments carry over to the present case of Coulomb gauge. A perturbative evaluation of the ghost-gluon vertex in Coulomb gauge shows indeed that its quantum corrections are finite and independent of the scale [7,25].

The vacuum expectation value $\langle F_A \rangle$ is commonly expressed in terms of the Coulomb form factor f . This quantity measures the deviation of $\langle F_A \rangle$ from the factorized form $\langle G_A \rangle G_0^{-1} \langle G_A \rangle$ and is defined in momentum space by

$$F(\mathbf{p}) =: G(\mathbf{p})f(\mathbf{p})\mathbf{p}^2 G(\mathbf{p}), \quad (116)$$

where $G = \langle G_A \rangle$ is the ghost propagator (23). By taking the vacuum expectation value of the operator identity

$$F_A = \frac{\partial}{\partial g}(gG_A), \quad (117)$$

the Coulomb form factor $f(\mathbf{p})$ can be related to the ghost form factor $d(\mathbf{p})$ and from the ghost DSE (59) the following (approximate) integral equation for the Coulomb form factor is obtained [4,36]:

$$f(\mathbf{p}) = 1 + g^2 \frac{N_c}{2} \int d\mathbf{q} \frac{1 - (\hat{\mathbf{p}} \cdot \hat{\mathbf{q}})^2}{\Omega(\mathbf{q})} (\mathbf{p} - \mathbf{q})^2 \times G^2(\mathbf{p} - \mathbf{q})f(\mathbf{p} - \mathbf{q}). \quad (118)$$

In the derivation of this equation no assumption on the form of the vacuum wave functional enters, so this equation remains also valid for non-Gaussian wave functionals.

With the approximation $\tilde{\Gamma}$ [Eq. (35)] $\rightarrow \tilde{\Gamma}_0$ [Eq. (16)], Eqs. (59), (106), and (118) form a closed set of coupled equations for the ghost propagator $G(\mathbf{p})$, the gluon energy $\Omega(\mathbf{p})$, and the Coulomb form factor $f(\mathbf{p})$, whose solutions provide the variational solution of the Yang-Mills Schrödinger equation. These equations have to be renormalized, which can be done in exactly the same way as in Refs. [4,12,29]. The numerical solution of this set of equations can be carried out as in the case of the Gaussian wave functional [4,8] and is subject to future work.

As already mentioned before, the use of a Gaussian wave functional misses the contribution of the bare three-gluon vertex and thus the gluon loop in the gap equation. Fortunately, as we have seen in the previous subsection, the gluon loop is IR subleading compared to the (included) ghost loop and thus irrelevant for the IR behavior of the Green functions. Therefore the results of Refs. [4,8] remain fully valid in the IR. In particular, the gluon propagator does not change in the IR. The gluon loop does, however, matter in the UV and is responsible for the anomalous dimension of the gluon propagator, which enters the running coupling constant.

VII. THE THREE- AND FOUR-GLUON VERTICES

As we have seen, the gap equation differs from the one obtained in [4] only by the gluon-loop contribution, which gives sizable corrections in the midmomentum regime. In the present section, we investigate the three- and four-gluon vertices $\Gamma_{3,4}$ by using the ghost and gluon propagators determined with a Gaussian wave functional [8] as input. We will not resort to the tree-level result $\Gamma_n = \gamma_n$ but rather solve the corresponding DSEs to one-loop order.

A. Solution of the truncated three-gluon-vertex DSE

The DSE for the three-gluon vertex at one-loop order is given by Eq. (55). Assuming ghost dominance (see, for example, Ref. [6]), we keep only the ghost loop [the third term on the right-hand side of Eq. (55) and Fig. 9]. Furthermore, we replace the full ghost-gluon vertex by the bare one; see Sec. VIC. After extracting the color

structure, the truncated DSE for the three-gluon vertex becomes

$$\Gamma_{ijk}(\mathbf{p}, \mathbf{q}, \mathbf{k}) = \gamma_{ijk}(\mathbf{p}, \mathbf{q}, \mathbf{k}) + ig^3 N_c \times \int d\ell G(\ell) G(\ell - \mathbf{p}) G(\ell + \mathbf{q}) \ell_i \ell_j (\ell - p)_k, \quad (119)$$

where momentum conservation $\mathbf{k} + \mathbf{p} + \mathbf{q} = 0$ is implied and we have omitted longitudinal terms, which, by definition, cannot enter the proper n -point vertex functions (36) of the transverse (Coulomb) gauge field. Possible tensor decompositions of the three-gluon proper vertex are given in Refs. [37,38]. Here, for sake of illustration, we confine ourselves to the form factor corresponding to the tensor structure of the bare three-gluon vertex, defined by

$$f_{3A} := \frac{\Gamma_3^{(0)} \circ \Gamma_3}{\Gamma_3^{(0)} \circ \Gamma_3^{(0)}}, \quad (120)$$

where $\Gamma_3^{(0)}$ is the perturbative vertex given in Eq. (101). Restricting the kinematic configuration to the case where two external momenta have the same magnitude, i.e.,

$$\mathbf{q}^2 = \mathbf{p}^2 = p^2, \quad \mathbf{q} \cdot \mathbf{p} = cp^2, \quad (121)$$

the form factor Eq. (120) depends only on two variables, the magnitude p of the two momenta and the cosine c of the angle between them. Contracting Eq. (119) with the bare three-gluon vertex [Eq. (101)], thereby using the variational kernel γ_3 [Eq. (100)] and the tensor structure T_3 given in Eq. (66a), yields the following equation for the form factor f_{3A} Eq. (120):

$$f_{3A}(p^2, c) = \frac{2p + \sqrt{2p^2(1+c)}}{2\Omega(p^2) + \Omega(2p^2(1+c))} - g^2 \frac{N_c}{4} \frac{2 + \sqrt{2(1+c)}}{p(1-c)(9+8c+c^2)} \times \int d\ell G(\ell) G(\ell - \mathbf{p}) G(\ell + \mathbf{q}) \mathcal{B}(\ell, \mathbf{p}, \mathbf{q}), \quad (122)$$

where we have introduced the abbreviation

$$\mathcal{B}(\ell, \mathbf{p}, \mathbf{q}) = \ell^2 [p^2(1-c) - (1+2c)(\ell \cdot \mathbf{q} - \ell \cdot \mathbf{p})] + \frac{(\ell \cdot \mathbf{q})^3}{p^2} - \frac{(\ell \cdot \mathbf{p})^3}{p^2} - (1+c)[(\ell \cdot \mathbf{q})^2 + (\ell \cdot \mathbf{p})^2] + (\ell \cdot \mathbf{q})(\ell \cdot \mathbf{p}) \left[c(1+c) + 2 + \frac{1-c}{p^2} (\ell \cdot \mathbf{q} - \ell \cdot \mathbf{p}) \right]. \quad (123)$$

The apparent singularity at $c = 1$ in the coefficient in front of the integral in Eq. (122) is cancelled by the numerator, and the whole term is regular in the collinear limit. Also the singularities at $\ell = 0$, $\ell = \mathbf{p}$, and $\ell = -\mathbf{q}$ are integrable.

For the actual calculation of f_{3A} [Eq. (120)], we use the numerical result for $\Omega(\mathbf{p})$ and $G(\mathbf{p})$ obtained in Ref. [8] (with a Gaussian wave functional) as input. For $\Omega(\mathbf{p})$ we

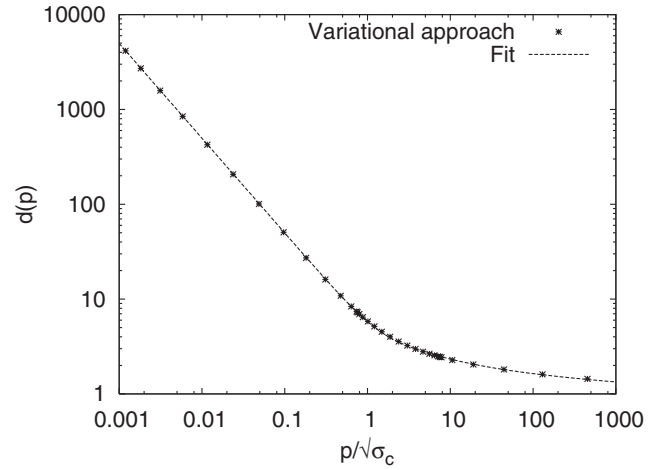


FIG. 18. Ghost form factor from [8] and fit to Eq. (124).

use the parametrization equation (113) while the ghost form factor $d(\mathbf{p}) = \mathbf{p}^2 G(\mathbf{p})$ is parametrized as

$$d(x) = a \sqrt{\frac{1}{x^2} + \frac{1}{\ln(x^2 + c^2)}}, \quad x^2 = \frac{\mathbf{p}^2}{\sigma_c}, \quad (124)$$

with σ_c being the Coulomb string tension. The fit to the data shown in Fig. 18 yields $a \approx 5$ and $c \approx 4$.

The form (124) of the ghost form factor embodies also the nonperturbative anomalous dimension, which in turn guarantees the convergence of the integral in Eq. (122).

The numerical results for $f_{3A}(p^2, c)$ are shown in Fig. 19 for some values of the cosine of the relative angle, c . The logarithmic plot (left panel) shows that the curves for different c have the same power law behavior in the infrared region, namely, p^{-3} , in agreement with the IR analysis of the ghost loop carried out in Ref. [38], according to which the IR exponent of the form factor f_{3A} should be 3 times the one of the ghost dressing function [Eq. (124)].⁵ The linear plot (right panel) shows that the form factor approaches unity in the high-momentum regime and changes sign in the midmomentum regime.

In Ref. [39] the form factor f_{3A} Eq. (120) of the three-gluon vertex was evaluated on the lattice for $d = 3$ Yang-Mills theory in Landau gauge. The result is shown in Fig. 20 and compares well to our result in low-momentum regime. In particular, in both studies, the sign change of the form factor occurs roughly at the same momentum where the gluon propagator has its maximum. The $d = 3$ Yang-Mills theory in Landau gauge can be interpreted as using the wave functional

$$\psi[A] = \mathcal{N} \exp \left[-\frac{1}{4\mu^2} \int (F_{ij}^a)^2 \right] \quad (125)$$

⁵In Ref. [6], due to the use of a Gaussian wave functional, the bare term escaped, and only the ghost loop was calculated for a different solution of the DSEs [4], which leads to less IR singular ghost and gluon propagators.

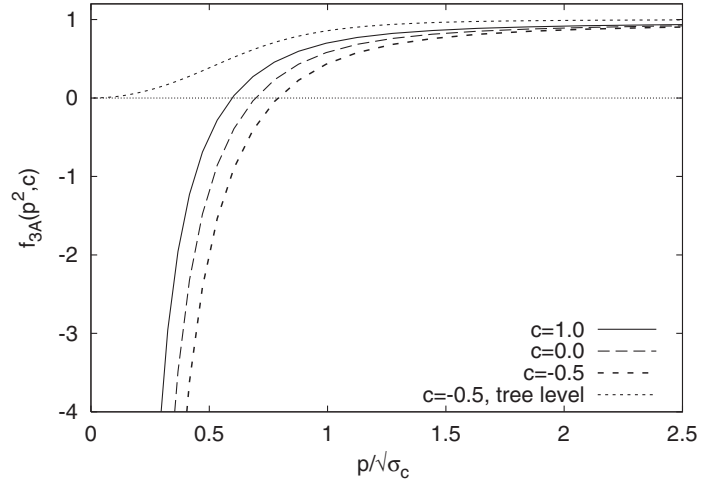
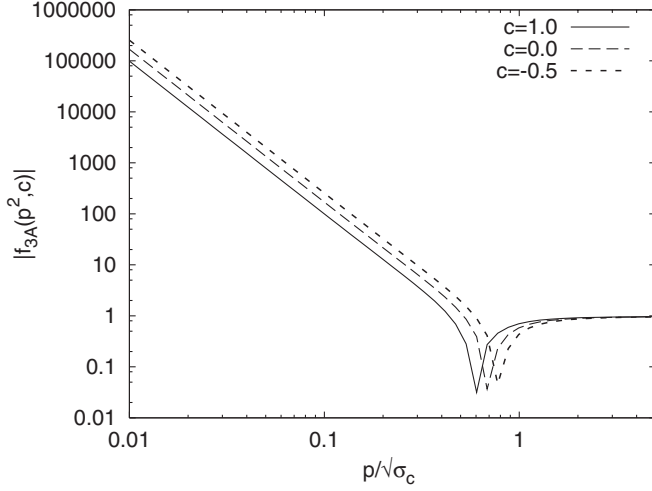


FIG. 19. Form factor $f_{3A}(p^2, c)$ defined in Eq. (120) for two momenta of equal magnitude p plotted for various values of the relative angle c .

in the Hamiltonian approach to $d = 3 + 1$ Yang-Mills theory in Coulomb gauge. This wave functional can be considered to represent the strong coupling limit of the true vacuum wave functional [40]. In Ref. [41] it was shown by means of lattice calculations that this wave functional yields static propagators which in the IR compare well with those obtained in $d = 3 + 1$ Yang-Mills theory in Coulomb gauge. Thus we can conclude from Fig. 20 that our results compare favorably with the lattice data.

B. Estimate of the four-gluon vertex

Because of its DSE (56), the four-gluon vertex is given in leading order (neglecting loops) by the variational kernel γ_4 [Eq. (104)] determined in Sec. VI A. A form factor for

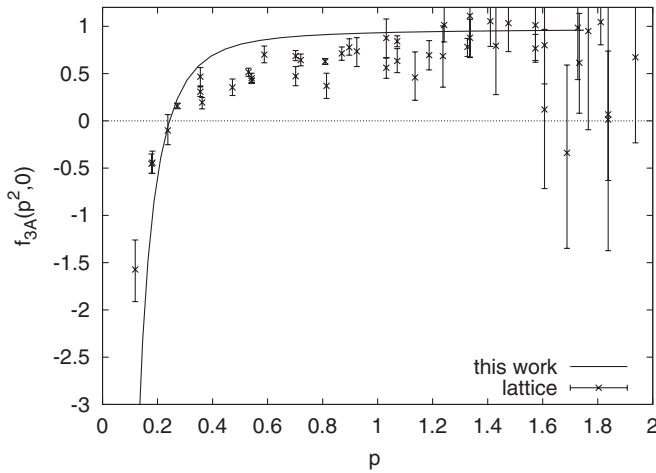


FIG. 20. Form factor f_{3A} of the three-gluon vertex for orthogonal momenta and comparison to lattice data for the $d = 3$ Landau-gauge vertex [39]. The momentum scale is arbitrary and has been adjusted to make the sign change occur at the same point. The lattice data are shown courtesy of A. Maas.

the four-gluon vertex can be introduced along the same line of Eq. (120):

$$f_{4A} := \frac{\Gamma_4^{(0)} \circ \gamma_4}{\Gamma_4^{(0)} \circ \Gamma_4^{(0)}}, \quad (126)$$

where $\Gamma_4^{(0)}$ is the perturbative four-gluon vertex, which is obtained from Eq. (104) by the replacements $\Omega(\mathbf{p}) \rightarrow |\mathbf{p}|$, $F(\mathbf{p}) \rightarrow 1/\mathbf{p}^2$. We consider here the form factor f_{4A} at the symmetric point, where

$$\mathbf{p}_1^2 = \dots = \mathbf{p}_4^2 = p^2, \quad \mathbf{p}_i \cdot \mathbf{p}_j = -\frac{1}{3}p^2 \quad (i \neq j). \quad (127)$$

For this kinematic configuration the terms in Eq. (104) stemming from the Coulomb interaction do not contribute to this vertex, and one finds for the form factor (126)

$$f_{4A}(p^2) = \frac{p}{\Omega(p^2)} \times \frac{171 - 960[g_0 + g(p^2)] + 8704g_0g(p^2)}{171 - 1920g_0 + 8704g_0^2}, \quad (128)$$

where

$$g(p^2) = \left[\frac{p}{2\Omega(p^2) + \Omega(\frac{4}{3}p^2)} \right]^2, \quad (129a)$$

$$g_0 = g(p^2)|_{\Omega(p^2)=p} = \frac{3}{8}(2 - \sqrt{3}). \quad (129b)$$

The function f_{4A} [Eq. (128)] is shown in Fig. 21. The function multiplying $p/\Omega(p^2)$ in Eq. (128) is of $\mathcal{O}(1)$, and the form factor at the symmetric point [Eq. (127)] can be fairly well represented by the gluonic dressing function $p/\Omega(p^2)$ alone.

In the above calculation of the four-gluon vertex we have neglected all loop diagrams, in particular, the ghost loop.

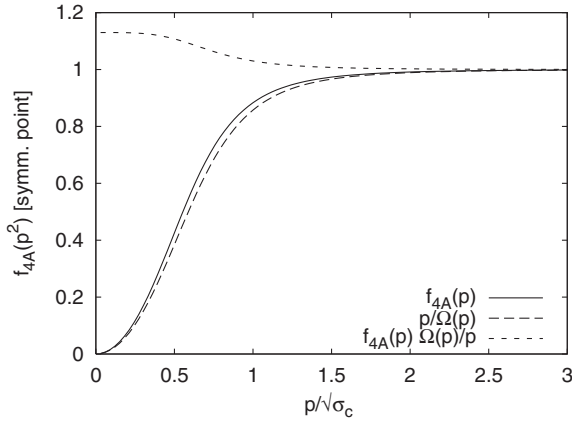


FIG. 21. Form factor $f_{4A}(p^2)$ of the four-gluon vertex at the symmetric point. The leading contribution $p/\Omega(p)$ is also shown.

From analogous investigations in Landau gauge [42] one may expect that the ghost loop dominates the IR behavior of the four-gluon vertex as it did for the three-gluon vertex. We will defer this issue to future research.

VIII. SUMMARY AND CONCLUSIONS

We have presented a general method to treat non-Gaussian wave functionals in the Hamiltonian formulation of quantum field theory. By means of well-established Dyson-Schwinger equation techniques, the equal-time Green functions and, in particular, the expectation value of the Hamiltonian are expressed in terms of kernels occurring in the exponent of the vacuum wave functional. These kernels are then determined by the variational principle minimizing the vacuum energy density. The method was applied to Yang-Mills theory in Coulomb gauge using a vacuum wave functional which contains up to quartic terms in the exponent. In leading order (in the number of loops) the cubic and quartic interaction kernels obtained from the variational principle are reminiscent of the

corresponding expressions obtained in leading order of a perturbative solution of the Yang-Mills Schrödinger equation, except that the unperturbed gluon propagators are replaced by the full ones. We have estimated these interaction kernels $\gamma_{3,4}$ and the corresponding proper gluon-vertex functions $\Gamma_{3,4}$ by using the gluon and ghost propagators found in the variational approach with a Gaussian wave functional. The resulting three-gluon vertex compares fairly well to the available lattice data obtained in $d = 3$ Landau gauge. The (gap) equation of motion obtained from the variation of the energy density with respect to the gluon propagator contains the gluon loop, which was missed in previous variational approaches due to the use of a Gaussian wave functional. We have shown that the gluon loop gives a substantial contribution in the mid-momentum regime while leaving the IR sector unchanged. Furthermore (together with the contribution from the non-Abelian Coulomb interaction already fully included in previous studies [4]), it also provides the correct asymptotic UV behavior of the gluon propagator in accord with perturbation theory [7]. The approach developed in the present paper allows a systematic treatment of correlations in the Hamiltonian approach to interacting quantum field theories (analogous to the so-called “exponential S ” method in many-body physics) and opens up a wide range of applications. In particular, it allows us to extend the variational approach from pure Yang-Mills theory to full QCD. This will be subject to future research.

ACKNOWLEDGMENTS

The authors are grateful to P. Watson and J.M. Pawłowski for useful discussions and for a critical reading of the manuscript. They also thank A. Maas for providing the lattice data for the three-gluon vertex shown in Fig. 20. This work has been supported by the Deutsche Forschungsgemeinschaft (DFG) under Contract No. DFG-Re856-3 and by the Cusanuswerk-Bischöfliche Studienförderung.

-
- [1] J. Greensite, *Prog. Part. Nucl. Phys.* **51**, 1 (2003).
 - [2] A.P. Szczepaniak and E.S. Swanson, *Phys. Rev. D* **65**, 025012 (2001).
 - [3] A.P. Szczepaniak, *Phys. Rev. D* **69**, 074031 (2004).
 - [4] C. Feuchter and H. Reinhardt, *Phys. Rev. D* **70**, 105021 (2004); arXiv:hep-th/0402106.
 - [5] H. Reinhardt and C. Feuchter, *Phys. Rev. D* **71**, 105002 (2005).
 - [6] W. Schleifenbaum, M. Leder, and H. Reinhardt, *Phys. Rev. D* **73**, 125019 (2006).
 - [7] D.R. Campagnari, H. Reinhardt, and A. Weber, *Phys. Rev. D* **80**, 025005 (2009).
 - [8] D. Epple, H. Reinhardt, and W. Schleifenbaum, *Phys. Rev. D* **75**, 045011 (2007).
 - [9] G. Burgio, M. Quandt, and H. Reinhardt, *Phys. Rev. Lett.* **102**, 032002 (2009).
 - [10] A. Yamamoto and H. Suganuma, *Phys. Rev. D* **81**, 014506 (2010).
 - [11] D.R. Campagnari and H. Reinhardt, *Phys. Rev. D* **78**, 085001 (2008).
 - [12] H. Reinhardt and D. Epple, *Phys. Rev. D* **76**, 065015 (2007).
 - [13] M. Pak and H. Reinhardt, *Phys. Rev. D* **80**, 125022 (2009).
 - [14] H. Reinhardt, *Phys. Rev. Lett.* **101**, 061602 (2008).

- [15] D. Zwanziger, *Nucl. Phys.* **B518**, 237 (1998).
- [16] V.N. Gribov, *Nucl. Phys.* **B139**, 1 (1978).
- [17] S. Mandelstam, *Phys. Rep.* **23**, 245 (1976).
- [18] G. 't Hooft, *Nucl. Phys.* **B190**, 455 (1981).
- [19] M. Leder, J.M. Pawłowski, H. Reinhardt, and A. Weber, [arXiv:1006.5710](https://arxiv.org/abs/1006.5710).
- [20] F.J. Dyson, *Phys. Rev.* **75**, 1736 (1949).
- [21] J.S. Schwinger, *Proc. Natl. Acad. Sci. U.S.A.* **37**, 452 (1951).
- [22] C. Itzykson and J.B. Zuber, *Quantum Field Theory* (McGraw-Hill, New York, 1980).
- [23] D. Zwanziger, *Nucl. Phys.* **B412**, 657 (1994).
- [24] P. Watson and H. Reinhardt, *Phys. Rev. D* **77**, 025030 (2008).
- [25] D. Campagnari, A. Weber, H. Reinhardt, F. Astorga, and W. Schleifenbaum, [arXiv:0910.4548](https://arxiv.org/abs/0910.4548).
- [26] W.J. Marciano and H. Pagels, *Phys. Rep.* **36**, 137 (1978).
- [27] N.H. Christ and T.D. Lee, *Phys. Rev. D* **22**, 939 (1980).
- [28] P. Watson and H. Reinhardt, *Phys. Rev. D* **76**, 125016 (2007).
- [29] D. Epple, H. Reinhardt, W. Schleifenbaum, and A.P. Szczepaniak, *Phys. Rev. D* **77**, 085007 (2008).
- [30] K. Langfeld, H. Reinhardt, and J. Gattnar, *Nucl. Phys.* **B621**, 131 (2002).
- [31] C.S. Fischer, A. Maas, and J.M. Pawłowski, *Ann. Phys. (N.Y.)* **324**, 2408 (2009).
- [32] C. Popovici, P. Watson, and H. Reinhardt, *Phys. Rev. D* **81**, 105011 (2010).
- [33] J.C. Taylor, *Nucl. Phys.* **B33**, 436 (1971).
- [34] A. Cucchieri, T. Mendes, and A. Mihara, *J. High Energy Phys.* **12** (2004) 012.
- [35] A. Sternbeck, E.M. Ilgenfritz, M. Müller-Preussker, and A. Schiller, *Nucl. Phys. B, Proc. Suppl.* **153**, 185 (2006).
- [36] A.R. Swift, *Phys. Rev. D* **38**, 668 (1988).
- [37] J.S. Ball and T.-W. Chiu, *Phys. Rev. D* **22**, 2550 (1980).
- [38] R. Alkofer, M.Q. Huber, and K. Schwenzer, *Eur. Phys. J. C* **62**, 761 (2009).
- [39] A. Cucchieri, A. Maas, and T. Mendes, *Phys. Rev. D* **77**, 094510 (2008).
- [40] J. Greensite, *Nucl. Phys.* **B158**, 469 (1979); *Phys. Lett. B* **191**, 431 (1987).
- [41] M. Quandt, H. Reinhardt, and G. Burgio, *Phys. Rev. D* **81**, 065016 (2010).
- [42] C. Kellermann and C.S. Fischer, *Phys. Rev. D* **78**, 025015 (2008).